DESCRIPTION AND QUATERNARY HISTORY OF THE CAMPO GRANDE FAULT OF THE HUECO BASIN, HUDSPETH AND EL PASO COUNTIES, TRANS-PECOS TEXAS

by

Edward W. Collins and Jay A. Raney

Final Contract Report

Prepared for

Texas Low-Level Radioactive Waste Disposal Authority
Under Interagency Contract Number IAC(90-91)0268

by

Bureau of Economic Geology
W. L. Fisher, Director
The University of Texas at Austin
Austin, Texas 78713

January 1990

CONTENTS

List of Figures

Appendix Figures

List of Tables

Plates (in pocket)

ABSTRACT

The Hueco Basin of Trans-Pecos Texas and Chihuahua, Mexico, formed in response to Basin and Range extensional tectonism that began about 24 Ma ago and continues to the present. The southeastern arm of the basin is asymmetrical with the thickest sediments deposited along the fault-bounded basin axis near the southwestern flank. Approximately 45 km long and striking northwestward, the Campo Grande fault is 12 km from the northeastern basin edge; it divides the downthrown, central part of the basin (>2,000 m of fill) from the shallower (175 m of fill) northeastern flank. Another major northwest-striking fault dips northeastward and bounds the southwestern basin margin in Mexico.

The Campo Grande fault trend is composed of en echelon fault strands that are 1.5 to 10 km long and have strikes of N25° to 75°W. Dips are between 60° and 90° southwest. Displacements decrease near terminations of strands. Grooves on fault planes indicate mostly dip-slip movement. Fault scarps have been modified by erosion of the footwall and deposition on the hanging wall. Erosion-resistant caliche (stages IV to V) at the surface aids in preserving scarp heights of between 1.5 and 11.5 m and scarp slopes of 4° to 17°.

Analysis of faulted upper Tertiary and Quaternary units indicates that successively younger units have less displacement. Maximum vertical offset measured across fault strands cutting the middle Pleistocene Madden Gravel (0.6 to 0.4 Ma old), which caps the Camp Rice Formation, is about 10 m. Repeated arroyo incision and fluvial aggradation since the middle Pleistocene have developed Pleistocene terraces that are locally correlative and are mapped as parts of the regionally outcropping Ramey and Balluco Gravels. Holocene terraces also occur. Maximum throws across fault strands that cut Ramey terraces (0.4 to 0.1 Ma old?) are 2.5 to 3 m, but some Ramey deposits overlie fault strands and are not faulted. Offset of Balluco (0.1 to 0.025 Ma old?) and Holocene terraces has not been observed at fault strands that cut Ramey terraces. The average recurrence interval is 0.1 Ma (maximum), and the last faulting episode was late Pleistocene. On the

downdropped block of one fault strand, faulted calcic horizons (0.5 to 1.0 m thick; stage III) with vertical separations of 1 to 2 m indicate at least five episodes of movement, deposition, and surface stabilization during the last 0.6 to 0.4 Ma. Maximum vertical offset during the last faulting event was about 1 to 1.5 m.

INTRODUCTION

The Campo Grande fault is a major fault zone in the southeastern Hueco Basin, or Hueco Bolson, of Trans-Pecos Texas (fig. 1). This zone is composed of a series of en echelon normal faults. Quaternary strata are offset and scarps are expressed at the surface along the fault trend. Documentation of the history of fault movement is important because an area 1.2 to 3.1 mi (2 to 5 km) northeast of the fault is being studied as a site for a proposed low-level radioactive waste repository (fig. 1). Data on Quaternary faulting are important for assessing potential earthquake hazards and for designing a safe repository (Slemmons and dePolo, 1986). Knowledge of the Campo Grande fault also provides information on the development of the Hueco Basin and on the history of Basin and Range faulting in the region. This report describes the fault in detail and discusses the Quaternary history of fault movement. Interpretations are based on scarp investigations and analysis of crosscutting relationships between the fault strands and Quaternary units. The fault is best exposed between Alamo and Diablo Arroyos, 1.8 to 4.6 mi (3 to 7.5 km) northeast of Fort Hancock (figs. 1, 2a, and plate 1), and it is this portion of the fault trend that was studied in most detail.

The Hueco Basin of Trans-Pecos Texas and Chihuahua, Mexico, lies within the northern Chihuahuan Desert and has a subtropical arid climate. Annual mean precipitation is approximately 20 to 23 cm and mean temperature is about 17°C (Orton, 1969, p. 33, 39; National Climatic Data Center, 1985, p. 15). Plants most common in the desert study area are creosote bush (*Larrea tridentata*), tar bush (*Flourensia cernua*), cat claw (*Acacia greggi*), and mesquite (*Prosopis juliflora*).

Methods

Study results are based on geologic mapping, field observations, and measurements of fault scarps, outcrops, excavations, and shallow (9 m maximum) augerholes. Most outcrops are along arroyos and gullies. Selected field stations are illustrated in figure 2 and table 1. Most of the aerial photographs interpreted for this study were low-sun-angle morning and afternoon photographs at approximate scales of 1:12,000 and 1:6,000, taken during December 1985. Smaller scale (approximately 1:62,000) and older (1953) Army Mapping Survey aerial photographs were also examined. U.S. Geological Survey 7.5-minute topographic quadrangle maps (1:24,000) include the Small, Campo Grande, Diablo Canyon West, Cavett Lake, Fort Hancock NW, Tornillo, and Clint SE Quadrangles. Geologic mapping was done at scales of 1:12,000 and 1:6,000. Detailed profiles of scarps were measured using an Abney level. Five excavations were dug by bulldozer, and nine shallow augerholes were drilled (three by trailer-mounted rig and six by portable power auger). Approximately 85 days were spent collecting field data between June 1988 and May 1989.

Previous Work

A northwest-striking fault strand southwest of Campo Grande Mountain and a fault scarp northwest of this mountain were first mapped by Albritton and Smith (1965) during regional studies of the Sierra Blanca area. They stated that the westernmost fault extended northwestward out of their study area and reported seeing no evidence of faulting in any gravels younger than the Madden Gravel (table 2) within their regional study area. Strain (1966) also mapped a northwest-striking fault in this region between Camp Rice and Diablo Arroyos during his stratigraphic investigations of the Fort Hancock and Camp Rice Formations. He reported the fault may offset these basin-fill deposits by as much as 60 m. A short fault strand was also mapped southwest of Campo Grande Mountain by Willingham (1980) during his study of the basin-fill deposits. Part of

the Campo Grande fault is shown on the Geologic Atlas of Texas, Van Horn–El Paso Sheet, scale 1:250,000 (Dietrich and others, 1983) and on the Tectonic Map of Rio Grande Rift Region in New Mexico, Chihuahua, and Texas, scale 1:1,000,000 (Woodward and others, 1978). A recent report prepared by Sergent, Hauskins, and Beckwith (1989) also illustrates and discusses the Campo Grande fault. Characteristics of the Campo Grande fault mentioned in the Sergent, Hauskins, and Beckwith (1989) report were formally presented by Barnes and others (1989a). Other Quaternary faults of the Hueco Basin have been mapped or described by Muehlberger and others (1978), Woodward and others (1978), Seager (1980), Henry and Gluck (1981), Henry and Price (1985), Machette (1987), Sergent, Hauskins, and Beckwith (1989), Barnes and others (1989b), and Keaton and others (1989). Other research on Quaternary faults in parts of Trans-Pecos Texas and central and southern New Mexico includes works by Goetz (1977, 1980), Machette (1978a,b), Seager (1981), Gile (1987), and Beehner (1989). Geologic maps of parts of northwestern Mexico (Coordinacion General De Los Servicios Nacionales De Estadistica, Geografia E Informatica), scale 1:250,000, were also used during this study.

TECTONIC SETTING

The Hueco Basin is an intermontane basin that formed in response to Basin and Range faulting that was initiated about 24 Ma ago. An earlier deep sedimentary basin, the Chihuahua Trough, developed during the Jurassic Period in westernmost Trans-Pecos Texas and in Chihuahua, Mexico (Henry and Price, 1985). The northeastern margin of the trough approximately parallels the present Rio Grande on the Texas side of the river and probably consists of down-to-the-southwest normal faults. This northwest-trending part of the Hueco Basin coincides with the regional structure zone referred to as the Texas Lineament (Muehlberger, 1980). Jurassic evaporites are the oldest Chihuahua Trough deposits. Cretaceous marine sediments filled this basin and buried the trough-bounding normal faults (Henry and Price, 1985). The Clint fault (Uphoff, 1978), interpreted from subsurface data collected 18.6 mi (30 km) southeast of El Paso, verifies

the existence of one of these normal faults that bound the Chihuahua Trough. Subsequent Laramide deformation thrust Cretaceous rocks northeastward along a décollement zone of Jurassic evaporites and produced north-northwest-trending thrust faults, folds, and monoclines along the northeastern margin of the Chihuahua Trough (Gries and Haenggi, 1971; Henry and Price, 1985). The Krupp No. 1 Thaxton well that was drilled in the study area (plate 1) encountered a thrust fault in Cretaceous bedrock at 420 m below the surface. The northeastern edge of the Laramide thrust faults is interpreted from seismic data to be approximately 2.5 to 3 mi (4 to 5 km) northeast of the trace of the Campo Grande fault.

Volcanic activity in the Trans-Pecos region occurred from about 48 to 17 Ma ago, although most of the activity was between 38 and 28 Ma ago (Henry and McDowell, 1984; Henry and Price, 1984, 1985; Henry and others, 1986). The nearest volcanic rocks are basaltic, andesitic, and trachytic to latite dikes and sills of the Finlay Mountains, about 4.3 to 9.3 mi (7 to 15 km) east-northeast of the study area and basalt intrusions, about 9.3 mi (15 km) southeast of the study area (fig. 1). Dates of the Finlay Mountain intrusions range between 46 and 50 Ma (Matthews and Adams, 1986; Henry and others, 1986), and the basalts southeast of the study area are about 29 and 34 Ma (Henry and others, 1986). The domed outcrop pattern of the Permian and Cretaceous rocks exposed in the Finlay Mountains suggests that two large igneous bodies are present in the subsurface (Albritton and Smith, 1965; Matthews and Adams, 1986). Most of the volcanism in Trans-Pecos Texas occurred while the area was under east-northeast compression during the waning stages of Laramide deformation (Price and Henry, 1984; Henry and Price, 1985). A transition to regional tension occurred about 30 Ma ago, and subsequent normal faulting related to Basin and Range extension was well developed by about 24 Ma ago (Henry and Price, 1985, 1986; Stevens and Stevens, 1985). Basin and Range faulting and magmatism in Trans-Pecos Texas and southern New Mexico has been episodic (Seager and others, 1984; Henry and Price, 1985; Stevens and Stevens, 1985). In Trans-Pecos Texas periods of accelerated fault movement and sediment deposition in structural troughs may have occurred between 24 to 17 Ma ago, about 10 Ma ago, and after 7 Ma ago (Stevens and Stevens, 1985, their fig. 4). Early regional extension

was oriented east-northeast, and later extension was oriented northwest (Henry and Price, 1985; Price and others, 1985). Although evidence of this change in extension directions in the Trans-Pecos region has been interpreted, the time of this shift has not been well established. A similar change in stress field orientation occurred in other parts of the Basin and Range Province about 10 Ma ago (Henry and Price, 1985).

Seager (1980) described the northwestern part of the Hueco Basin (northwest of the study area) as an asymmetric, west-tilted graben. Mattick (1967) calculated as much as 2,740 m of basin fill in the center of the graben at the northwestern arm of the basin; Ramberg and others (1978) estimated between 2,000 and 3,000 m of Cenozoic fill. The geometry of the Hueco Basin in the study area is also asymmetric. Wen (1983) determined that basin fill along the basin axis southwest of the Campo Grande fault was greater than 2,000 m thick. Gravity and magnetic maps presented by Keller and Peeples (1985) also outline an area of thick basin-fill southwest of the Campo Grande fault. Northeast of the fault, boreholes intersected the base of the basin-fill sediments at depths of about 175 m.

The Campo Grande and other normal faults of the Hueco Basin formed during Basin and Range extension. LeMone (1989) interpreted the northwest-striking subsurface Mesozoic Clint fault, as defined by Uphoff (1978), as being related to the similarly striking Campo Grande fault. Uphoff (1978), however, clearly shows in a cross section that the Clint fault does not offset the Cenozoic bolson fill. In addition, north-striking Quaternary faults trend through the area between the Campo Grande and Clint faults. Although it is possible that the Campo Grande fault is related to Basin and Range reactivation of a preexisting fault, there is no evidence that it is continuous with the Clint fault.

Most of the historical seismicity of Trans-Pecos Texas has occurred near the north-trending Salt Basin region, approximately 56 mi (90 km) east of the Campo Grande fault study area (Sanford and Toppozada, 1974; Dumas, 1980; Reagor and others, 1982; Davis and others, 1989). No events have been reported along the Campo Grande fault, although Dumas (1980, his fig. 1) plots two epicenters along the Texas–Mexico border in the Hueco Basin, including one located

near the northwestern end of the Campo Grande fault. Dumas reported that these epicenter locations are accurate to within 5 mi (8 km). Most historical earthquakes of the Hueco Basin have been near El Paso; the largest event was a Modified Mercalli (MM) intensity VI. The 1931 Valentine earthquake (Dozier, 1987) of intensity VII MM (M=6.4) located near Valentine, Texas, about 62 mi (100 km) southeast of the study area, is the largest recorded earthquake in Trans-Pecos Texas.

STRATIGRAPHY

Stratigraphic nomenclature used in this report is based on the work of Albritton and Smith (1965) and Strain (1964, 1966) (table 2). Plate 1 illustrates that the surface geology in the vicinity of the Campo Grande fault comprises hills of Lower Cretaceous bedrock that are surrounded by Pliocene through Recent sediments.

Lower Cretaceous Units

Cretaceous units that crop out in the study area include (in ascending sequence) the Bluff Mesa Formation, Cox Sandstone, and Finlay Limestone. The Bluff Mesa is mostly limestone, although the unit also contains minor amounts of sandstone and shale. Cox is mostly sandstone with some limestone, and Finlay is dominantly limestone (Albritton and Smith, 1965). In the study area these units were fractured and folded during Laramide compressional deformation. Albritton and Smith (1965) mapped a syncline and an overturned anticline at Campo Grande Mountain (plate 1). About 4.3 to 6.2 mi (7 to 10 km) north of the study area, Cox Sandstone and Finlay Limestone crop out on the Diablo Plateau and its escarpment. On the plateau these units are relatively undeformed and flat lying, although at the plateau escarpment they gently dip 5° to 8° southwestward into the Hueco Basin, forming a west-northwest-striking monocline. This deformation possibly was caused by loading that occurred during the Laramide thrusting southwest

of the plateau. Later subsidence of the Hueco Basin may have also warped these Cretaceous rocks along the plateau escarpment (basin flank). Seismic data indicate that Cretaceous strata beneath basin-fill sediments between the escarpment and the thrust margin also dip southwestward at low angles. Approximately 2.5 mi (4 km) north of the study area, a borehole encountered Washita rocks below the basin-fill sediments. Cretaceous Finlay Limestone, Cox Sandstone, and Campagrande Formation and Permian rocks in the Finlay Mountains (3.1 mi [5 km] northeast of the study area) have been domed upward by igneous intrusions.

Pliocene to Pleistocene Fort Hancock and Camp Rice Formations

The Fort Hancock and Camp Rice Formations of the Hueco Basin were initially defined by Strain (1964, 1966). These formations have also been referred to by Albritton and Smith (1965) as older and younger basin fill. More recent investigations of these units in Trans-Pecos Texas and south-central New Mexico include descriptions by Hawley and others (1969), Strain (1971), Willingham (1980), Riley (1984), Stuart and Willingham (1984), Vanderhill (1986), and Gustavson (1989). Fort Hancock sediments that crop out in the study area are clay, silt, and sand; bedded gypsum and gravel are locally present elsewhere in the unit but are rarely found in the study area. Sediments composing the Fort Hancock Formation were deposited in a bolson setting. Camp Rice Formation sand and gravel, with lesser silt and clay, represent alluvial fan, fluvial, minor lacustrine, and floodplain deposition. Braided stream deposits near the basin axis were deposited by the ancestral Rio Grande after it developed as a through-flowing stream. Camp Rice sediments unconformably overlie the Fort Hancock Formation, but in many areas the contact is subtle because of similarities in lithologic composition and depositional setting. At a locality southwest of the fault, Vanderhill (1986) determined the contact to be about 2.48 Ma old on the basis of paleomagnetic studies. Volcanic ash lenses within the Camp Rice aid in determining its age (tables 2 and 3). Ash present in outcrops in Diablo Arroyo (in the study area) and Madden Arroyo (3.1 mi [5 km] southeast of the study area) are within the lower part of the Camp Rice Formation

and have been reported as the 2.1-Ma-old Huckleberry Ridge ash by Gile and others (1981) and Izett and Wilcox (1982). The 0.6-Ma-old Lava Creek B ash has been reported by these researchers to crop out at the top of the Camp Rice Formation near El Paso, Texas, about 37 mi (60 km) northwest of the study area.

Pleistocene Gravel Units

Albritton and Smith (1965) defined and regionally mapped five Pleistocene gravel units that overlie the Fort Hancock and Camp Rice Formations in the Hueco Basin. Oldest to youngest, they are the Miser, Madden, Gills, Ramey, and Balluco Gravels. Geologic mapping by Albritton and Smith (1965) indicates Madden, Ramey, and Balluco Gravels are regionally extensive deposits, whereas the Miser and Gills Gravels occur only locally. Madden, Ramey, and Balluco Gravels have been mapped in the study area by the authors (plate 1). The gravel units were deposited on piedmont slopes and on terraces of arroyos that have incised older sediments. Gravel is locally derived and, in the study area, the pebbles and cobbles consist mostly of limestone, sandstone, andesite, and chert. These units are usually 1.5 to 2.5 m thick, and the calcic soils and indurated calcic soils (referred to in this report as caliche) that are developed within and that cap these units are 0.5 to 1.5 m thick.

Characteristics of calcic soils have been described by Gile and others (1966, 1981) and Machette (1985). Machette (1985) described several processes that could precipitate calcic soils, favoring a process that involves airborne $CaCO_3$ and Ca^{+2} dissolved in rainwater. The $CaCO_3$ particles, which are leached from the surface and upper horizons of the soil, precipitated in lower soil horizons at a depth controlled by soil moisture and texture (Machette, 1985; McFadden and Tinsley, 1985). Morphologic stages of $CaCO_3$ in calcic soils and pedogenic caliche developed under arid and semiarid climates in the American Southwest have been described by Gile and others (1966) and Machette (1985). Six stages of sequential $CaCO_3$ development (numbered I through VI) are defined on the basis of physical characteristics. In this classification, Madden

Gravel caliche is mostly stage IV because of its development of thin to thick laminae in the upper part of the horizon and the presence of laminae that drape over fractured surfaces. Stage V, which is characterized by thick laminae and carbonate-coated fractures, has developed locally. Ramey Gravel caliche is mostly stage IV to III, which is determined by the massive $CaCO_3$ accumulations existing between clasts where gravel content is high and by a matrix that is firmly to moderately cemented where gravel content is low. Sparse laminae also occur in the upper part of the Ramey Gravel caliche. Locally, Ramey Gravel caliche is less developed and is stage III to II. It is characterized by a firmly cemented matrix with slight to massive $CaCO_3$ accumulations between clasts and by coatings on tops and undersides of pebbles or, where gravel content is low, by a matrix that is weakly cemented. Balluco Gravel calcic soils are usually at stage II development, which is characterized by continuous, thin to thick $CaCO_3$ coatings on the tops and undersides of pebbles. Local calcic soils developed in alluvium on the downthrown blocks of several fault strands have stage III development, as indicated by coalesced nodules and a firmly to moderately cemented matrix.

Miser Gravel does not exist in the study area, and only small, well-dissected remnant deposits adjacent to the Quitman Mountains were mapped by Albritton and Smith (1965). Miser Gravel appears to be a fan facies of the Madden piedmont gravel. Madden Gravel is more regionally extensive than the Miser, and in the study area Madden Gravel caps a piedmont slope on the Camp Rice Formation. Gills Gravel is not mapped in the study area. Regional mapping by Albritton and Smith (1965) identified the Gills only locally near Arroyo Calero, about 10.5 mi (17 km) southeast of Diablo Arroyo. The Ramey and Balluco Gravels of the fault study area were deposited on terraces of Diablo, Camp Rice, and Alamo Arroyos, which have incised Madden Gravel and the older Camp Rice and Fort Hancock Formations (plate 1 and fig. 3). Southeast of the study area, adjacent to the Quitman Mountains, Ramey and Balluco Gravels were deposited on piedmont slopes.

Presumed ages of the Pleistocene gravel units are estimates based on field stratigraphic relationships, the degree of calcic soil development, and possible correlation with similar units in

New Mexico. The possible age ranges are illustrated in table 2. These units lack suitable materials for accurate age dating. Albritton and Smith (1965) interpreted the Miser Gravel to be the oldest gravel unit on the basis of its elevation. In their map area, it is present only locally adjacent to the Quitman Mountains; this field characteristic prevents regional correlation of the unit. The regionally extensive Madden Gravel appears to correlate with the LaMesa and Jornada I surfaces of south-central New Mexico. The 0.6-Ma-old Lava Creek B ash in the upper Camp Rice Formation provides a maximum age. In south-central New Mexico, the LaMesa surface is overlain by basalt dated at about 0.5 Ma. Calcic soils of the Madden, Gills, Ramey, and Balluco Gravels have decreasing morphologic stages of $CaCO_3$ development, respectively. Field relationships indicate that the Balluco Gravel, the youngest gravel unit, is older than terraces of the modern Rio Grande (fig. 3). The last major episode of Rio Grande entrenchment occurred approximately 25,000 to 10,000 years ago (Gile and others, 1981).

Holocene Alluvium and Windblown Sand

Arroyo and gully alluvium, similar to the Pleistocene gravel units, is composed of locally derived sand and gravel. Modern arroyo channel deposits and young low terraces were mapped together during this study (plate 1). Carbonized wood in Alamo Arroyo alluvium has been dated as being 970 $\pm$ 20 years old (tables 2 and 3). Organic material found in low terrace alluvium in upper Alamo Arroyo has been dated as being 1,330 $\pm$ 60 years old. Both of these dated samples were collected north of the fault study area. Organic material in alluvial slope deposits overlying the Madden or Ramey Gravel also was collected about 2.8 mi (4.5 km) north of the study area and has been dated as being 3,240 $\pm$ 330 and 7,510 $\pm$ 100 years old. Windblown sand forms stabilized low dunes and coppice mounds that cover the Madden, Ramey, and Balluco Gravels over much of the study area.

FAULT OCCURRENCE AND GEOMETRY

The Campo Grande fault is a 45-km-long fault trend that is composed of at least 16 en echelon fault strands (fig. 2). This series of faults strikes northwestward, is downthrown toward the southwest, and is about 7.5 mi (12 km) from the northeastern edge of the Hueco Basin. The Campo Grande fault divides the downthrown, central part of the basin (>2,000 m of fill) from the shallower (175 m of fill) northeastern flank. In the footwall of the Campo Grande fault are several northwest-trending limestone and sandstone (Cretaceous bedrock) hills. The Campo Grande fault was named after Campo Grande Mountain, the highest of the hills that are adjacent to the fault strands (Strain, 1966). The fault is the southwest margin of a narrow, 2- to 4-km-wide, bedrock high (possibly a horst block) (fig. 3 and plate 1). Seismic data locally indicate that the northeast margin of this bedrock high may be fault bounded, although the inferred northeast-dipping normal fault does not cut Fort Hancock sediments (>2.48 Ma old) exposed at the surface.

Individual fault strands are 1.5 to 10 km long and have strikes of N25° to 75°W (figs. 2 and 4a). Dips are between 60° and 90° southwest. Outcrops and excavations of the faults indicate that smaller displacement (offsets commonly less than 1 m) faults are commonly adjacent to the main fault strands (plates 2a and b; appendix figs. A-1, A-2, and A-4). These main fault strands commonly displace Fort Hancock sediments against Camp Rice sediments. Gentle warping and tilting of strata adjacent to faults is common. At a few locations in the footwall block, the units gently dip (as high as 7°) toward the fault. Units in the hanging-wall block locally dip as much as 10° toward the fault, although at several locations units dip 5° to 15° away from the fault. Pebbles and cobbles of the coarser units are commonly rotated immediately adjacent to the fault planes.

Although the Tertiary and Quaternary sediments that crop out are not strongly lithified, grooves that formed during fault movement are present on some of the main fault planes and indicate slip direction. These grooves have rakes of 65° to 90° (fig. 4b). The main component of movement on these normal faults is in a downdip direction. Some of the measurements that have a

small oblique-slip component probably result from dip slip on fault planes that curve along strike. Thus, some parts of the curved normal faults are not perpendicular to extension direction. The strike of one curving fault trace changes from N12°W to N42°W to N74°W along 0.2 km, and the strikes of many faults shift by about 25° over short distances. Small-displacement faults (throws <1 m) strike between N°34 to 60°W and dip 49° to 88° southwest and northeast. They typically form small grabens and horsts. Grooves on the main fault planes and the geometries of small-scale grabens and horsts indicate that the normal faults developed by extension in a N30° to 40°E to S30° to 40°W direction (fig. 4b and c). Sediments along fault planes are often cemented with $CaCO_3$. Soft-sediment deformation that possibly is due to liquefaction initiated by earthquakes has been observed at only one location 1,300 ft (400 m) south of station 44 (fig. 2b). This deformation is characterized by chaotic folds in Camp Rice sand (fig. 5) and possible fluid-escape structures. Timing of this event is unknown, but it clearly occurred when the Camp Rice sediments were water saturated.

SCARP MORPHOLOGY

Analyses of fault-scarp morphologies have been used to interpret approximate absolute ages of young normal faults in the western United States (Wallace, 1977; Bucknam and Anderson, 1979; Nash, 1980; Machette, 1982, 1987; Mayer, 1984; Personius and Machette, 1984; Machette and others, 1986). Qualitative and quantitative analyses of scarp slopes with scarp heights are often used to estimate ages of the last faulting event. The basis for assuming a relationship between scarp morphology and scarp age is that scarps formed by high-angle faults are nearly vertical and degrade by initial collapse of the scarp face and subsequent erosion and deposition along the scarp (Wallace, 1977). Bucknam and Anderson (1979) determined that for scarps of known age, scarp-slope angles increase at regular increments when scarp heights increase. Degradation of scarps through time (increasing scarp ages) results in lower scarp-slope angles.

The duration of erosion is a major factor that influences the morphology of fault scarps, although climate and lithology also affect scarp erosion and are equally important. Regional and local variations in climate or temporal changes in climate may affect how rapidly scarps erode. Scarps of similar ages that are eroded under dissimilar climatic conditions may have different morphologies, or scarps of different ages could have similar morphologies. Highly localized climate events and local physiographic settings may also cause variable erosion rates and thus cause significant variations in the morphology of a single fault scarp. Lithologies of the faulted units also directly influence rates of scarp erosion. In the Campo Grande fault study area, surface and near-surface caliche (commonly stage IV, locally stage V) overlies relatively unconsolidated sediments, provides some resistance to erosion, and significantly affects the development of scarp morphology.

Scarp Descriptions

Scarps of the Campo Grande fault trend have been modified by erosion of the footwall and deposition on the hanging wall. In many places windblown sand also covers the scarps, preventing detailed observations. The scarps are mostly single-slope scarps (fig. 6a), although in a few isolated areas compound scarps that have multiple scarp-slope angles (Wallace, 1977) are present (fig. 6a and b). Single-slope scarp heights range between 1.5 and 11.5 m, and scarp slopes are between 3° and 11°, although slopes are most commonly 4 to 6° (fig. 7 and table 4). Steeper slopes of the compound scarps are 10° and 17° and are up to 1.7 m high. The regional surface slopes 1° to 3° southwestward, perpendicular to the strike of the fault scarps. Heights of scarps (particularly those on the Madden Gravel surface) commonly do not accurately indicate amounts of fault offsets because of deposition of sediments over the faulted horizon on the hanging-wall block.

Scarps of the Campo Grande fault trend are less distinct (have smaller slope angles) than some of the other faults of the Hueco Basin. Scarps of faults that are at the base of Sierra De San Ignacio, Sierra De La Amargosa, and Sierra San Jose Del Prisco, in Chihuahua, Mexico (17 mi

[28 km] southwest of the Campo Grande fault at the southwest margin of the Hueco Basin), have slope angles up to 27° for 5- to 12-m-high scarps. A fault at the eastern base of the Franklin Mountains (within and north of El Paso) also has 5- to 12-m-high scarps that slope between 18° and 25° (Machette, 1987). These higher slope angles suggest that these faults were more recently active than the Campo Grande fault, or that erosion of these scarps has been slower than erosion of the Campo Grande fault.

Scarp of Fault Strand G

The most distinct scarp associated with the Campo Grande fault trend is the scarp of fault strand G (figs. 2a and 8). This scarp is 2.5 km long and strikes N55° to 60°W. A 2-km section between stations 1 and 29 (fig. 2b) was studied in detail to document the variations in morphologic characteristics along an individual scarp and to provide data concerning relative scarp age and faulting history.

Sedimentologic variations along the scarp are illustrated in plates 2a and b (excavation stations are shown in fig. 2b). Madden Gravel caliche (commonly stage IV), gravel, and sand are at the surface or near the surface at the scarp crest and top of the footwall block. The southwestward regional surface slope of the Madden Gravel is only 1° to 3°. Lithologies present on the surface of the scarp slope are gravel consisting of caliche pebbles, and pebbles and cobbles of limestone, sandstone, and andesite that are typical of the Madden Gravel in this area. Locally along the scarp slope, caliche crops out. The caliche horizon either dips almost parallel to the scarp slope or it is eroded. Surface sediments at the base of the scarp are alluvial sand with scattered pebbles of limestone, sandstone, andesite, and caliche.

The scarp is well dissected (figs. 8 and 9), and intermittent streams that have incised some of the larger gullies that cut the scarp have deposited fanlike alluvial sediments on the hanging-wall block (plate 1). Windblown sand deposits commonly cover the surface on the hanging-wall block and, at a few localities, cover parts of the scarp and footwall block (plate 1). Some of the gullies

that cross the scarp are as broad as 30 to 100 m and are filled with alluvium that is being incised by narrower (1.5- to 2.5-m-wide) channels. The recent alluvium is not faulted, and many of the modern gully channels are more deeply incised on the hanging-wall block than on the footwall block.

Scarp slopes and heights vary appreciably along the fault strand (figs. 9 and 10). Heights range from 1.5 to 6.5 m. The different heights are attributed mostly to variations in the amounts of alluvial deposition on the hanging wall and to erosion on the footwall block, although differences in fault offset may also occur. Higher scarp heights near station 29 (fig. 9) probably result from erosion of sediments of the hanging-wall block by a drainage into nearby (0.6 mi [1 km] west) Camp Rice Arroyo.

This scarp of fault strand G has a single slope of 4° to 7° in most places, although at several localities compound slopes exist. Steep sections of the compound slopes are as much as 17° (fig. 11 and table 4). Areas with compound slopes appear to be better protected from erosion caused by gullying and sheetwash across the Madden Gravel surface. The steepest scarp slope is at station 14, which is protected from erosion by limestone hills located up the regional slope that divert some drainage away from the station. Figure 10 illustrates the subtle character of most of the scarp of fault strand G.

Excavations Across Scarp of Fault Strand G

Logs of three excavations that were dug across the scarp of fault strand G are illustrated in plates 2a and b. An excavation at station 14 (excavation 14) intersects a part of the fault strand that has a compound scarp (steep slope angle as much as 17°), and excavations at stations 25 and 8 (excavations 25 and 8) intersect relatively distinct (7° slope angle) and subtle (4° slope angle) single-slope scarps, respectively. The excavations uncovered a main fault striking approximately N60°W and dipping 70° to 85° southwest as well as adjacent smaller displacement normal faults having offsets generally less than 0.5 m. Smaller displacement faults are in the footwall block; they

strike N34° to 60°W and dip 49° to 88° southwest and northeast, forming small grabens and horsts. The main fault at excavation 14 intersects the surface at the steep section of the compound-slope scarp, between the scarp base and crest. At excavations 25 and 8, which cut single-slope scarps, the main fault projects to the ground surface about 6 to 7 m southwest of the scarp base. Smaller scale faults do not appear to intersect the surface and often appear to terminate at or within the 1- to 1.5-m-thick surface to near-surface caliche horizon (commonly stage IV) of the Madden Gravel. Fractures having no offset occur in the caliche. Most of the fractures that are within 20 m of the main fault strike approximately parallel to the fault. Some fractures are filled with sand and silt, and a few are wedge shaped, indicating they have opened due to horizontal extension caused by flexing or warping of the caliche horizon.

Scarp slopes at excavations 25 and 8 and the more gently dipping portion of the compound-slope scarp at excavation 14 are underlain by the Madden Gravel caliche horizon, which appears to dip the same amount as the scarp slopes. The caliche may have formed on the slope, or it may have been gently warped during faulting. A combination of gentle warping and precipitation of caliche on the slope also may have occurred. At excavations 25 and 8, the upper contact of the Madden Gravel caliche beneath alluvium southwest of the scarp base has been eroded.

In the hanging wall of the fault are five faulted calcic horizons (stage III) that are 0.5 to 1.0 m thick (plate 2a). These horizons have vertical separations of 1 to 2 m. The deepest and oldest calcic horizon is within the downdropped Madden Gravel, which has been offset about 10 m. The uppermost calcic horizon is clearly faulted at excavation 14 (1.4 m throw), and the physical characteristics of this calcic soil (stage III carbonate morphology) suggest that it may have taken about 100,000 years for this $CaCO_3$ horizon to develop (Machette, 1985, p. 11). The upper calcic horizon at excavation 25 is interpreted as being the same upper horizon as that in excavation 14, although the configuration of the more subtle scarp slope makes offset difficult to verify. The upper calcic horizon at excavation 8 is interpreted as being younger than the upper calcic horizons identified in excavations 14 and 25. This interpretation is based on the observation that the sediments at excavation 8 are only very slightly carbonate cemented. A much smaller amount of

carbonate has accumulated in this horizon than in the upper calcic horizons in excavations 14 and 25. This slightly calcic horizon at excavation 8 does not appear to be faulted. Thick windblown sand deposits at excavation 8 may account for the additional young sediments that are not present at excavations 14 and 25.

Unconsolidated sand, silt, and gravel overlying the faulted upper calcic horizon at excavation 14 are in lateral contact with the main fault plane and upthrown Madden Gravel caliche (plate 2a). These unconsolidated sediments are interpreted as having been deposited as slope wash rather than as having been faulted against the caliche. This caliche is sufficiently resistant to erosion to have remained coherent during deposition of these sediments. The gravel unit overlying the upper calcic horizon at the east wall of this excavation is a localized deposit that does not extend to the west wall, 11 ft (3.5 m) away. The east wall was excavated along a narrow (approximately 1- to 2-m-wide) gully that apparently transported the gravel only a short distance to the downdropped block. The gully also causes slight variation in the shape of the scarp at the east and west walls of excavation 14.

Scarp Morphology and Fault Age

The ages of Campo Grande fault scarps have not been quantitatively estimated using the morphologic data because erosion-resistant caliche and possible climate differences prevent quantitative comparison of the Campo Grande fault scarps with age-calibrated scarp-morphology data determined by Bucknam and Anderson (1979) and Machette (1982) from scarps in unconsolidated sediments in Utah and New Mexico. Even though caliche may slow scarp degradation, Campo Grande fault scarps have smaller slope angles than scarps with similar heights in Utah and New Mexico that have been dated as Holocene and latest Pleistocene in age. This rough comparison suggests that the Campo Grande fault scarps may be late or middle Pleistocene.

Evidence of multiple fault movements includes the compound-slope scarps that have been preserved at a few localities and the buried calcic soil horizons on the downdropped fault block.

The last episode of fault movement occurred long enough ago to allow erosion to degrade most of the scarps to a single slope and to entrench small valleys across the fault scarp and fill them with alluvium, which is currently being incised. The overlying calcic horizons on the downdropped fault block indicate at least five episodes of movement, deposition, and surface stabilization on this fault. A more detailed discussion of faulting history appears later in this report (p. 24).

CROSSCUTTING RELATIONSHIPS BETWEEN STRATIGRAPHY AND FAULTS

The crosscutting relationships between stratigraphic units and faults were used to interpret average rates of fault movement and to bracket the time of the most recent fault movement. Average rates of fault movement were determined by comparing the amounts of displacement on units of different age. The time of most recent fault movement was estimated by comparing the ages of the youngest faulted unit with the oldest unfaulted units. Camp Rice sediments are downdropped against Fort Hancock sediments along the extent of the Campo Grande fault trend. The total displacement of these units is the cumulative offset across one to three fault strands. Throws on younger Quaternary units are small enough to measure across individual fault strands. Measurements of throws and vertical separations (fig. 6c) are similar in these very gently dipping (<3°) units. The geologic map (plate 1) of the study area illustrates in plan view the crosscutting relationships between the faults and the stratigraphic units.

Fort Hancock–Camp Rice Contact and Faults

The contact between the Fort Hancock and Camp Rice Formations, approximately 2.48 Ma old (Vanderhill, 1986), is the oldest horizon offset by the Campo Grande fault that can be mapped in the study area. Lithologic differences between the two units and unit descriptions made by previous researchers (Strain, 1966; Willingham, 1980) aided in mapping the contact, which is subtle in some areas (plate 1). Strain's work (1966) and our own studies show the contact to be an

unconformity. The amount of erosion that has occurred on top of the Fort Hancock Formation, especially on the footwall block, is unknown; thus, the calculated offset values are regarded as minimum values.

In the vicinity of Diablo and Camp Rice Arroyos, cumulative vertical offset of the Fort Hancock–Camp Rice contact across the fault trend is about 44 m. In these areas the Fort Hancock–Camp Rice contact on the footwall block is more subtle than in other areas. There is little evidence of enhanced downcutting of the Fort Hancock Formation near the faults, although silts and clays, probably derived from the Fort Hancock Formation, are interbedded with Camp Rice sands in the hanging-wall block and are inferred to indicate some erosion of Fort Hancock sediments in the footwall.

At Alamo Arroyo, cumulative vertical offset of the Fort Hancock–Camp Rice contact across the fault trend is about 28 m. The contact on the footwall block near the fault is a distinct angular unconformity (fig. 12) that is probably locally younger than the contact present on the hanging-wall block (plate 1), which is estimated at 2.48 Ma old. Fault relationships at the station 136 outcrop, located on one of the two fault strands near Alamo Arroyo, indicate that (1) several episodes of faulting occurred during Camp Rice deposition, (2) this unconformity developed on downfaulted Camp Rice sediments as well as on upthrown Fort Hancock strata, and (3) only 1 m of offset has occurred at this locality since deposition on top of the unconformity (fig. A-3). The sand above the unconformity at station 136 is interpreted as being Camp Rice Formation, but the alternate interpretation that it is post–Camp Rice in age cannot be disregarded.

Madden Gravel and Faults

Throws of the Madden Gravel (0.6 to 0.4 Ma old) on different fault strands are summarized in table 5. At fault strands A, B, and E (fig. 2) the vertical offsets were not measured because windblown sand covers the Madden Gravel. However, the presence of linear sand-covered scarps in areas known to be underlain by Madden Gravel indicates that vertical displacement of the

Madden Gravel has occurred. Throws of 8 to 10 m (maximum) were measured at fault strands C, D, G, and J. Six meters of throw were measured at strand H, but because the Madden Gravel on the downdropped block dips 5° to 7° southwestward (away from the fault), the vertical separation of the faulted Madden Gravel is greater than 10 m if measured beyond the area of tilted sediments adjacent to the fault plane. Fault strand F has 1.3 m of throw at one location, but throws across this fault may be greater toward the northwest, where a scarp is covered by windblown sand. Throw is 1 to 2 m at strand L, and strands I and K do not intersect Madden Gravel.

Measurements indicate that throws may vary along fault strands. For example, at fault strand D, throws of 10 and 3.7 m were measured at stations 96 and 45, respectively (fig. 2). At fault strand G, the throw on the Madden Gravel is 9 to 10 m at several locations along the fault, but near the mappable eastern termination the throw is only 1 to 1.5 m.

Ramey Gravel and Faults

Faults H and I are the only strands that displace the Ramey Gravel (0.4 to 0.1 Ma old?); throws are 2.6 to 3 m (fig. 2 and table 5). Figure 13 illustrates the displacement of Ramey Gravel at station 35, fault strand H. Fort Hancock and Camp Rice sediments are more complexly faulted than Ramey Gravel because more faulting events have disrupted the older sediments. Faults D, J, K, and L do not displace the Ramey Gravel, as indicated by the presence of unfaulted Ramey overlying the faults and the absence of scarps. Appendix figure A-1 illustrates unfaulted Ramey Gravel overlying fault strand L. The absence of scarps on the Ramey that overlies fault strands A and B (fig. 2a) indicates that these faults do not offset this unit. Strands E, F, and G (fig. 2a) do not intersect Ramey Gravel. Fault relationships indicate that not all fault strands have ruptured during post-Ramey faulting events.

Balluco Gravel and Faults

Balluco Gravel (0.1 to 0.025 Ma old?) is the oldest unfaulted unit in the study area (table 5). Figure 14 illustrates an excavation at station 82 (excavation 82), fault strand H (fig. 2a), where unfaulted Balluco Gravel overlies a fault contact between Fort Hancock and Camp Rice sediments. Fault strands A, D, I, and L also are overlain by unfaulted Balluco Gravel, as indicated by an absence of scarps. Other fault strands do not intersect Balluco Gravel.

Alluvium and Faults

Similar to the Balluco Gravel, young gully and arroyo alluvium (0.025 Ma old? to present) also is unfaulted. At several outcrops, including those at stations 117 and 139 (appendix figs. A-4a and b), unfaulted young alluvium overlies a fault contact between Fort Hancock and Camp Rice sediments. Alluvium commonly is present in channels eroded into the underlying older sediments at the fault plane (appendix figs. A-1, A-2a, and A-4a). Lithologic differences between the Fort Hancock and Camp Rice Formations or structural discontinuities in the sediments along the fault plane probably enhance incision at the faults. Narrow channels, some with nearly vertical sides, are also commonly cut into these units away from the faults (fig. 15; appendix fig. A-4a).

Young alluvium at the station 139 outcrop (appendix fig. A-4b) is unfaulted, although the other field relationships at this location (appendix fig. A-4b) are inconclusive, and it is difficult to determine whether or not gravel (of unknown age) has been faulted against the Fort Hancock sediments. The similarity between lithologies of the Camp Rice sediments and younger alluvium also make interpretation difficult. It is clear that young alluvial sand and gravel overlie the fault at station 139 (appendix fig. A-4b) and are not offset. The gravel adjacent to the fault contains clasts of $CaCO_3$-cemented Fort Hancock Formation that appear to have been eroded from the upthrown block of the fault. The gravel adjacent to the fault plane also is cut by a fracture (striking oblique to

the fault) that is filled with caliche, indicating that these sediments are old enough for caliche to have precipitated. Caliche in fractures cutting Pleistocene or younger gravels have not been noted elsewhere in the study area. Rotated pebbles were not observed adjacent the sharp, 71°- to 76°-dipping fault plane. Because nearby Ramey and Balluco Gravels overlie the same fault strand and are unfaulted, and because of the uncertain age and inconclusive relationship of the gravel to the fault plane, the outcrop at station 139 is not interpreted as being probable evidence of a "young" (post-Balluco) faulting event.

Calcic Horizons and Faults

Faulted calcic soil horizons were identified on the downdropped blocks of fault strands D and G (fig. 2a). Carbonate horizons are 0.5 to 1.0 m thick and have stage III morphology. Vertical separations range from 1.1 to 2.2 m (table 6, plates 2a and b). These calcic horizons are faulted and at the station 45 outcrop (fault strand D), the two overlying calcic horizons merge away from the faults and form a single horizon. The calcic horizons represent different episodes of fault movement, deposition, and surface stabilization. At both fault strands the oldest calcic horizon studied in the hanging wall is in the upper Madden Gravel (0.6 to 0.4 Ma old). At fault strand G, four faulted calcic units overlie this oldest horizon, indicating at least five episodes of movement (plate 2a, excavation 14). About 100,000 years is the estimated time needed for the near-surface, faulted calcic horizon at excavation 14 to have accumulated the carbonate typical of the stage III morphology (see "Excavations Across Scarp of Fault Strand G," p. 16). The smaller number of faulted calcic horizons at station 45, fault strand D, indicates either that fewer faulting events have caused rupture along this strand or that physical conditions have prevented development of the additional calcic soil horizons. The youngest faulted calcic horizon on the hanging wall at station 45, fault strand D, has 1.5 to 2.0 m of younger alluvium and windblown sand covering it, and its age is unknown. This horizon may not be equivalent to the youngest horizon at excavation 14, fault strand G.

SUMMARY OF FAULTING HISTORY

Multiple faulting events of the Campo Grande fault trend have offset Pliocene and Quaternary sediments. Field evidence of multiple faulting events includes the presence of (1) compound scarps, (2) overlying and faulted calcic soil horizons on the downdropped block, and (3) successively younger faulted units having less displacement. Grooves on fault planes indicate that mostly dip-slip movement has occurred. Vertical offsets of the Fort Hancock–Camp Rice contact (2.48 Ma old), Madden Gravel (0.6 to 0.4 Ma old), and Ramey Gravel (0.4 to 0.1 Ma old?) are 44, 10, and 3 m, respectively, indicating that average rates of movement have been relatively constant over the last 2.48 Ma. A surface to near-surface calcic soil horizon that is estimated to be about 0.1 Ma old is also faulted. This indicates probable post-Ramey Gravel fault movement on a fault strand that does not intersect the Ramey Gravel. Some fault strands are overlain by unfaulted Ramey Gravel, indicating that some fault strands of the 45-km-long Campo Grande fault trend did not behave similarly during the latest faulting event(s). Although seismic events over time have resulted in producing a fault zone with interrelated en echelon strands, not all faults ruptured in the most recent event(s), and the fault zone is probably seismically segmented.

Fault strands G, H, and I are the most recently active. None of these fault strands offset Balluco Gravel (0.1 to 0.025 Ma old?). The latest faulting episode was late Pleistocene, probably between 0.1 and 0.025 Ma ago. Faulted calcic horizons on the downdropped block of fault strand G indicate at least five episodes of movement, deposition, and surface stabilization during the last 0.6 to 0.4 Ma. The maximum average recurrence interval calculated for the last 0.6 to 0.4 Ma from data at fault strand G is about 0.15 to 0.08 Ma. Because some faults of the 45-km-long fault trend have not consistently displaced the same unit, recurrence intervals along parts of the fault trend may be somewhat different. Vertical separation of overlying calcic horizons and the steep sections of compound scarps indicate that maximum vertical offsets during single faulting events have been about 1.0 to 2.0 m and that the maximum throw during the latest event was about 1.0 to 1.5 m.

CONCLUSIONS

1. The Campo Grande fault is a 45-km-long series of en echelon normal faults that have had dip-slip displacement.
2. Single-slope scarps with slope angles between 4° and 6° are most common, although at a few locations compound scarps, having slopes as much as 17°, are preserved. Scarp heights range between 1.5 and 11.5 m. Heights of scarps commonly do not accurately indicate amounts of fault offset because alluvial and eolian sediments commonly cover the faulted horizon in the hanging wall. Quantitative estimates of the age of the fault scarps were not made, although the morphologies suggest that the scarps may be as old as late or middle Pleistocene.
3. Excavations across scarps illustrate that the single-slope scarps are underlain by caliche that dips approximately the same as the scarp slope. The upper surface of the caliche is often eroded. The caliche could have formed on the slope or it could have been gently warped during faulting. A combination of caliche warping and precipitation on the slope also may have occurred.
4. Some of the scarps represent multiple faulting events, as indicated by the presence of compound scarps, overlying and faulted calcic soil horizons on the downdropped block, and successively younger units having less displacement.
5. The youngest faulted unit is the Ramey Gravel (0.4 to 0.1 Ma old?), and the oldest unfaulted unit is the Balluco Gravel (0.1 to 0.025 Ma old?), indicating that the latest movement was during the late Pleistocene. Some fault strands that are overlain by Ramey Gravel have not ruptured Ramey sediments, indicating that during at least the latest faulting event(s) the entire Campo Grande fault zone has not ruptured as a single segment.
6. Five calcic soil horizons (stage III morphology) on the downdropped block of one fault strand indicate at least five episodes of movement, deposition, and surface stabilization on

this fault during the last 0.6 to 0.4 Ma. The maximum average recurrence interval is about 0.15 to 0.08 Ma. Vertical separation of overlying calcic horizons and the steep sections of compound scarps indicate that maximum vertical offsets during single faulting events have been about 1.0 to 2.0 m and that the maximum throw during the latest event was about 1.0 to 1.5 m. On the basis of 2.6 to 3.0 m of offset on the Ramey Gravel (0.4 to 0.1 Ma old?), two faulting events are interpreted as having occurred on some fault strands since Ramey sediments were deposited, indicating an average recurrence interval of 0.2 to 0.05 Ma.

7. Vertical offsets of the Fort Hancock–Camp Rice contact (2.48 Ma old), Madden Gravel (0.6 to 0.4 Ma old), and Ramey Gravel (0.4 to 0.1 Ma old?) are about 44, 10, and 3 m, respectively, indicating that average rates of movement have been relatively constant over the last 2.48 Ma.

ACKNOWLEDGMENTS

Funding for this research was provided by the Texas Low-Level Radioactive Waste Authority under Interagency Contract Number 90-008 IAC(90-91)-0268. We wish to thank the following staff members of the Bureau of Economic Geology, The University of Texas at Austin: T. F. Hentz, for editorial review of the report; C. D. Henry, S. E. Laubach, and T. C. Gustavson, who reviewed parts of this report; Steve Martel, who helped organize and collect data for the initial field work; R. W. Baumgardner, Jr., and T. C. Gustavson, who provided helpful comments during the data-collection phase of this research; and James Doss and D. H. Ortuño, who drilled the shallow augerholes for this study. Other BEG staff members who contributed to the publication of this report were Tari Weaver, Patrice Porter, Lynn N. Griffin, and Annie K. Kearns, who drafted illustrations under the direction of Richard L. Dillon; and Jamie H. Coggin, designer, and Bobby Duncan, editor.

Discussions with J. W. Hawley, New Mexico Bureau of Mines and Mineral Resources, and several geologists and consultants for Sergent, Hauskins, and Beckwith, Geotechnical Engineers, including J. R. Barnes, D. B. Slemmons, and Peizhen Zhang, were also useful.

REFERENCES

Albritton, C. C., Jr., and Smith, J. F., Jr., 1965, Geology of the Sierra Blanca area, Hudspeth County Texas: U.S. Geological Survey Professional Paper 479, 131 p.

Barnes, J. R., Peizhen Zhang, and Slemmons, D. B., 1989a, The Campo Grande fault zone: a source for focused ground motion at the proposed low-level radioactive waste disposal site, Hudspeth County, Texas (abs.): Association of Engineering Geologists Abstracts and Program, 32nd Annual Meeting, p. 50.

Barnes, J. R., Shlemon, R. J., and Slemmons, D. B., 1989b, The Amargosa fault: a previously unstudied major active fault in northern Chihuahua, Mexico (abs.): Association of Engineering Geologists Abstracts and Program, 32nd Annual Meeting, p. 50–51.

Beehner, T. S., 1989, Geologic and geomorphic analysis of the Organ Mountains fault scarp, south-central New Mexico (abs.): Association of Engineering Geologists Abstracts and Program, 32nd Annual Meeting, p. 51.

Bucknam, R. C., and Anderson, R. E., 1979, Estimation of fault-scarp ages from a scarp-height-slope-angle relationship: Geology, v. 7, no. 1, p. 11–14.

Davis, S. D., Pennington, W. D., and Carlson, S. M., 1989, A compendium of earthquake activity in Texas: The University of Texas at Austin, Bureau of Economic Geology Geological Circular 89-3, 27 p., 4 microfiche in pocket.

Dietrich, J. W., Owen, D. E., and Shelby, C. A., 1983, Van Horn–El Paso Sheet, V. E. Barnes, project director: The University of Texas at Austin, Bureau of Economic Geology, Geologic Atlas of Texas, scale 1:250,000.

Dozier, D. I., 1987, The 16 August 1931 Valentine, Texas, earthquake: evidence for normal faulting in West Texas: Bulletin of the Seismological Society of America, v. 77, p. 2005–2017.

Dumas, D. B., 1980, Seismicity in the Basin and Range province of Texas and northeastern Chihuahua, Mexico, *in* Dickerson, P. W., Hoffer, J. M., and Callender, J. F., eds., Trans-Pecos region, southeastern New Mexico and West Texas: New Mexico Geological Society 31st Annual Field Conference Guidebook, p. 77–81.

Gile, L. H., 1987, Late Holocene displacement along the Organ Mountains fault in southern New Mexico: New Mexico Bureau of Mines and Mineral Resources Circular 196, 43 p.

Gile, L. H., Peterson, F. F., and Grossman, R. B., 1966, Morphological and genetic sequences of carbonate accumulation in desert soils: Soil Science, v. 101, no. 5, p. 347–360.

Gile, L. H., Hawley, J. W., and Grossman, R. B., 1981, Soils and geomorphology in the Basin and Range area of southern New Mexico—guidebook to the Desert Project: New Mexico Bureau of Mines and Mineral Resources Memoir 39, 222 p.

Goetz, L. K., 1977, Quaternary faulting in Salt Basin graben, West Texas: The University of Texas at Austin, Master's thesis, 136 p.

————1980, Quaternary faulting in Salt Basin graben, West Texas, *in* Dickerson, P. W., and Hoffer, J. M., eds., Trans-Pecos region: New Mexico Geological Society 31st Annual Field Conference, p. 83–92.

Gustavson, T. C., 1989, Sedimentary facies, depositional environments, and paleosols of the late Tertiary Fort Hancock Formation and the Tertiary–Quaternary Camp Rice Formation, Hueco Bolson, West Texas: The University of Texas at Austin, Bureau of Economic Geology, contract report prepared for the Texas Low-Level Radioactive Waste Authority under Interagency Contract Number IAC(88-89)-0932.

Gries, J. G., and Haenggi, W. T., 1971, Structural evolution of the eastern Chihuahua Tectonic Belt, *in* Seewald, Ken, and Sundeen, Dan, eds., The geologic framework of the Chihuahua Tectonic Belt: West Texas Geological Society, p. 119–138.

Hawley, J. W., Kottlowski, F. E., Seager, W. R., King, W. E., Strain, W. S., and LeMone, D. V., 1969, The Santa Fe Group in south-central New Mexico border region: New Mexico Bureau of Mines and Mineral Resources Circular 104, p. 52–76.

Hawley, J. W., 1975, Quaternary history of Dona Ana County region, south-central New Mexico, *in* Seager, W. R., Clemons, R. E., and Callender, J. F., eds., Las Cruces country: New Mexico Geological Society 26th Annual Field Conference Guidebook, p. 139–140.

Henry, C. D., and Gluck, J. K., 1981, A preliminary assessment of the geologic setting, hydrology, and geochemistry of the Hueco Tanks geothermal area, Texas and New Mexico: The University of Texas at Austin, Bureau of Economic Geology Geological Circular 81-1, 48 p.

Henry, C. D., and McDowell, F. W., 1984, Geochronology of magmatism in the Tertiary volcanic field, Trans-Pecos Texas, *in* Price, J. G., Henry, C. D., Parker, D. F., and Barker, D. S., eds., Igneous geology of Trans-Pecos Texas—field trip guide and research articles: The University of Texas at Austin, Bureau of Economic Geology Guidebook 23, p. 99–122.

Henry, C. D., and Price, J. G., 1984, Variations in caldera development in the mid-Tertiary volcanic field of Trans-Pecos Texas: Journal of Geophysical Research, v. 89, no. B10, p. 8765–8786.

————1985, Summary of the tectonic development of Trans-Pecos Texas: The University of Texas at Austin, Bureau of Economic Geology Miscellaneous Map No. 36, scale 1:500,000, 8 p.

————1986, Early Basin and Range development in Trans-Pecos Texas and adjacent Chihuahua: magmatism and orientation, timing, and style of extension: Journal of Geophysical Research, v. 91, no. B6, p. 6213–6224.

Henry, C. D., McDowell, F. W., Price, J. G., and Smyth, R. C., 1986, Compilation of potassium-argon ages of Tertiary igneous rocks, Trans-Pecos Texas: The University of Texas at Austin, Bureau of Economic Geology Geological Circular 86-2, 34 p.

Izett, G. A., and Wilcox, R. E., 1982, Map showing localities and inferred distributions of the Huckleberry Ridge, Mesa Falls, and Lava Creek ash beds (Pearlette family ash beds) of Pliocene and Pleistocene age in the western United States and southern Canada: U.S. Geological Survey Miscellaneous Investigations Map I-1325, scale 1:4,000,000.

Jones, B. R., and Reaser, D. F., 1970, Geology of Southern Quitman Mountains, Hudspeth County, Texas: The University of Texas at Austin, Bureau of Economic Geology Geologic Quadrangle Map No. 39, scale 1:48,000, text, 24 p.

Keaton, J. R., Shlemon, R. J., Slemmons, D. B., Barnes, J. R., and Clark, D. G., 1989, The Amargosa fault: a major late Quaternary intra-plate structure in northern Chihuahua, Mexico (abs.): Geological Society of America, Abstracts with Programs, v. 21, no. 6, p. A148.

Keller, G. R., and Peeples, W. J., 1985, Regional gravity and aeromagnetic anomalies in West Texas, *in* Dickerson, P. W., and Muehlberger, W. R., eds., Structure and tectonics of Trans-Pecos Texas: West Texas Geological Society Publication 85-81, p. 101–105.

LeMone, D. V., 1989, Structural constraints for proposed Fort Hancock Low-Level Radioactive Waste Disposal Site (NTP-S34), southern Hudspeth County, Texas (abs.): American Association of Petroleum Geologists Bulletin, v. 73, no. 3, p. 380 (also note errata in v. 73, no. 9, p. 1141).

Machette, M. N., 1978a, Bernalillo County dump fault, *in* Hawley, J. W., ed., Guidebook to Rio Grande rift in New Mexico and Colorado: New Mexico Bureau of Mines and Mineral Resources Circular 163, p. 153–155.

————1978b, Dating Quaternary faults in the southwestern United States by using buried calcic paleosols: U.S. Geological Survey, Journal of Research, v. 6, no. 3, p. 369–381.

————1982, Quaternary and Pliocene faults in the La Jencia and southern part of the Albuquerque-Belen Basins, New Mexico: evidence of fault history from fault-scarp morphology and quaternary geology, *in* Wells, S. G., Grambling, J. A., and Callender, J. F., eds., Albuquerque country II: New Mexico Geological Society 33rd Annual Field Conference Guidebook, p. 161–169.

————1985, Calcic soils of the southwestern United States, *in* Weide, D. L., ed., Soils and Quaternary geology of the southwestern United States: Geological Society of America Special Paper 203, p. 1–21.

————1987, Preliminary assessment of paleoseismicity at White Sands Missile Range, southern New Mexico: evidence for recency of faulting, fault segmentation, and repeat intervals for major earthquakes in the region: U.S. Geological Survey Open-File Report 87-444, 46 p.

Machette, M. N., Personius, S. F., Menges, C. M., and Pearthree, P. A., 1986, Map showing Quaternary and Pliocene faults in the Silver City 1° x 2° Quadrangle and the Douglas 1° x 2° Quadrangle, southeastern Arizona and southwestern New Mexico: U.S. Geological Survey Miscellaneous Field Studies Map MF-1465-C, scale 1:125,000.

Matthews, W. K., and Adams, J. A. S., 1986, Geochemistry, age, and structure of the Sierra Blanca and Finlay Mountain intrusions, Hudspeth County, Texas, *in* Price, J. G., Henry, C. D., Parker, D. F., and Barker, D. S., eds., Igneous geology of Trans-Pecos Texas—field trip guide and research articles: The University of Texas at Austin, Bureau of Economic Geology Guidebook 23, p. 207–224.

Mattick, R. E., 1967, A seismic and gravity profile across the Hueco Bolson, Texas: U.S. Geological Survey Professional Paper 575-D, p. 85–91.

Mayer, Larry, 1984, Dating Quaternary fault scarps formed in alluvium using morphologic parameters: Quaternary Research, v. 22, no. 3, p. 300–313.

McFadden, L. D., and Tinsley, J. C., 1985, Rate and depth of pedogenic-carbonate accumulation in soils: formulation and testing of a compartment model, *in* Weide, D. L., ed., Soils and Quaternary geology of the Southwestern United States, Geological Society of America Special Paper 203, p. 23–41.

Muehlberger, W. R., 1980, Texas lineament revisited, *in* Dickerson, P. W., and Hoffer, J. M., eds., Trans-Pecos region, southwestern New Mexico and West Texas: New Mexico Geological Society 31st Annual Field Conference Guidebook, p. 113–121,

Muehlberger, W. R., Belcher, R. C., and Goetz, L. K., 1978, Quaternary faulting in Trans-Pecos Texas: Geology, v. 6, no. 6, p. 337–340.

Nash, D. B., 1980, Morphologic dating of degraded normal fault scarps: Journal of Geology, v. 88, no. 3, p. 353–360.

National Climatic Data Center, 1985, Texas, 1984: Asheville, North Carolina, National Oceanic and Atmospheric Administration, Climatological Data Annual Summary, v. 89, no. 13, 78 p.

Orton, R. B., 1969, Climates of the states—Texas: Washington, D.C., U.S. Department of Commerce, Environmental Data Center, Climatography of the United States No. 60-41, 46 p.

Personius, S. F., and Machette, M. N., 1984, Quaternary and Pliocene faulting in the Taos Plateau region, northern New Mexico, *in* Baldridge, W. S., Dickerson, P. W., Riecker, R. E., and Zidek, Jiri, eds., Rio Grande Rift—northern New Mexico: New Mexico Geological Society 35th Field Conference Guidebook, p. 83–90.

Price, J. G., and Henry, C. D., 1984, Stress orientations during Oligocene volcanism in Trans-Pecos Texas: timing the transition from Laramide compression of Basin and Range tension: Geology, v. 12, no. 4, p. 238–241.

Price, J. G., Henry, C. D., Standen, A. R., and Posey, J. S., 1985, Origin of silver-copper-lead deposits in red-bed sequences of Trans-Pecos Texas: Tertiary mineralization in Precambrian, Permian, and Cretaceous sandstones: The University of Texas at Austin, Bureau of Economic Geology Report of Investigations No. 145, 65 p.

Ramberg, I. B., Cook, F. A., and Smithson, S. B., 1978, Structure of the Rio Grande rift in southern New Mexico and West Texas based on gravity interpretation: Geological Society of America Bulletin, v. 89, no. 1, p. 107–123.

Reagor, B. G., Stover, C. W., Algermissen, S. T., 1982, Seismicity map of the state of Texas: Denver, Colorado, U.S. Geological Survey Miscellaneous Field Studies, map MF-1388, scale 1:1,000,000.

Riley, R., 1984, Stratigraphic facies analysis of the upper Santa Fe Group, Fort Hancock and Camp Rice Formations, far West Texas and south-central New Mexico: The University of Texas at El Paso, Master's thesis, 108 p.

Sanford, A. R., and Toppozada, T. R., 1974, Seismicity of proposed radioactive waste disposal site in southeastern New Mexico: New Mexico Bureau of Mines and Mineral Resources Circular 143, 15 p.

Seager, W. R., 1980, Quaternary fault system in the Tularosa and Hueco Basins, southern New Mexico and West Texas, *in* Dickerson, P. W., and Hoffer, J. M., eds., Trans-Pecos region, southwestern New Mexico and West Texas: New Mexico Geological Society 31st Annual Field Conference Guidebook, p. 131–135.

————1981, Geology of Organ Mountains and southern San Andres Mountains, New Mexico: New Mexico Bureau of Mines and Mineral Resources Memoir 36, 98 p.

Seager, W. R., Shafiqullah, M., Hawley, J. W., and Marvin, R. F., 1984, New K-Ar dates from basalts and the evolution of the southern Rio Grande rift: Geological Society of America Bulletin, v. 95, no. 1, p. 87–99.

Sergent, Hauskins, and Beckwith, Consulting Geotechnical Engineers, 1989, Preliminary geologic and hydrologic evaluation of the Fort Hancock site (NTP-S34), Hudspeth County, Texas for the disposal of low-level radioactive waste: SHB Job No. E88-4008B, prepared for Hudspeth County, Texas, Hudspeth County Conservation and Reclamation District No. 1, Hudspeth County Underground Water Conservation District No. 1, and El Paso County, Texas, p. 5-1–5-52.

Slemmons, D. B., and dePolo, C. M., 1986, Evaluation of active faulting and associated hazards, *in* Wallace, R. E., ed., Active tectonics: Washington, D.C., National Academy Press, Geophysics Study Committee, p. 45–62.

Stevens, J. B., and Stevens, M. S., 1985, Basin and Range deformation and depositional timing, Trans-Pecos Texas, *in* Dickerson, P. W., and Muehlberger, W. R., eds., Structure and tectonics of Trans-Pecos Texas: West Texas Geological Society Field Conference, Publication 85-81, p. 157–163.

Strain, W. S., 1964, Blancan mammalian fauna and Pleistocene formations, Hudspeth County, Texas: University of Texas at Austin, Ph.D. dissertation, 148 p.

————1966, Blancan mammalian fauna and Pleistocene formations, Hudspeth County, Texas: Austin, Texas Memorial Museum Bulletin No. 10, 55 p.

————1971, Late Cenozoic bolson integration in the Chihuahua tectonic belt, *in* Hoffer, J. M., ed., Geologic framework of the Chihuahua tectonic belt: West Texas Geological Society Publication 71-59, p. 167–173.

Stuart, C. J., and Willingham, D. L., 1984, Late Tertiary and Quaternary fluvial deposits in the Mesilla and Hueco bolsons, El Paso area, Texas: Sedimentary Geology, v. 38, p. 1–20.

Uphoff, T. L., 1978, Subsurface stratigraphy and structure of the Mesilla and Hueco bolsons, El Paso region, Texas and New Mexico: The University of Texas at El Paso, Master's thesis, 65 p.

Vanderhill, J. B., 1986, Lithostratigraphy, vertebrate paleontology, and magnetostratigraphy of Plio-Pleistocene sediments in the Mesilla Basin, New Mexico: The University of Texas at Austin, Ph.D. dissertation, 305 p.

Wallace, R. E., 1977, Profiles and ages of young fault scarps, north-central Nevada: Geological Society of America, v. 88, no. 9, p. 1267–1281.

Wen, Cheng-Lee, 1983, A study of bolson fill thickness in the southern Rio Grande Rift, southern New Mexico, West Texas and northern Chihuahua: The University of Texas at El Paso, Master's thesis, 73 p.

Willingham, D. L., 1980, Stratigraphy and sedimentology of the upper Santa Fe Group in the El Paso region, West Texas and south-central New Mexico: The University of Texas at El Paso, Master's thesis, 93 p.

Woodward, L. A., Callender, J. F., Seager, W. R., Chapin, C. E., Gries, J. C., Shaffer, W. L., and Zilinski, R. E., 1978, Tectonic map of Rio Grande rift region in New Mexico, Chihuahua, and Texas, *in* Hawley, J. W., ed., Guidebook to Rio Grande rift in New Mexico and Colorado: New Mexico Bureau of Mines and Mineral Resources Circular 163, sheet 2, scale 1:1,000,000.

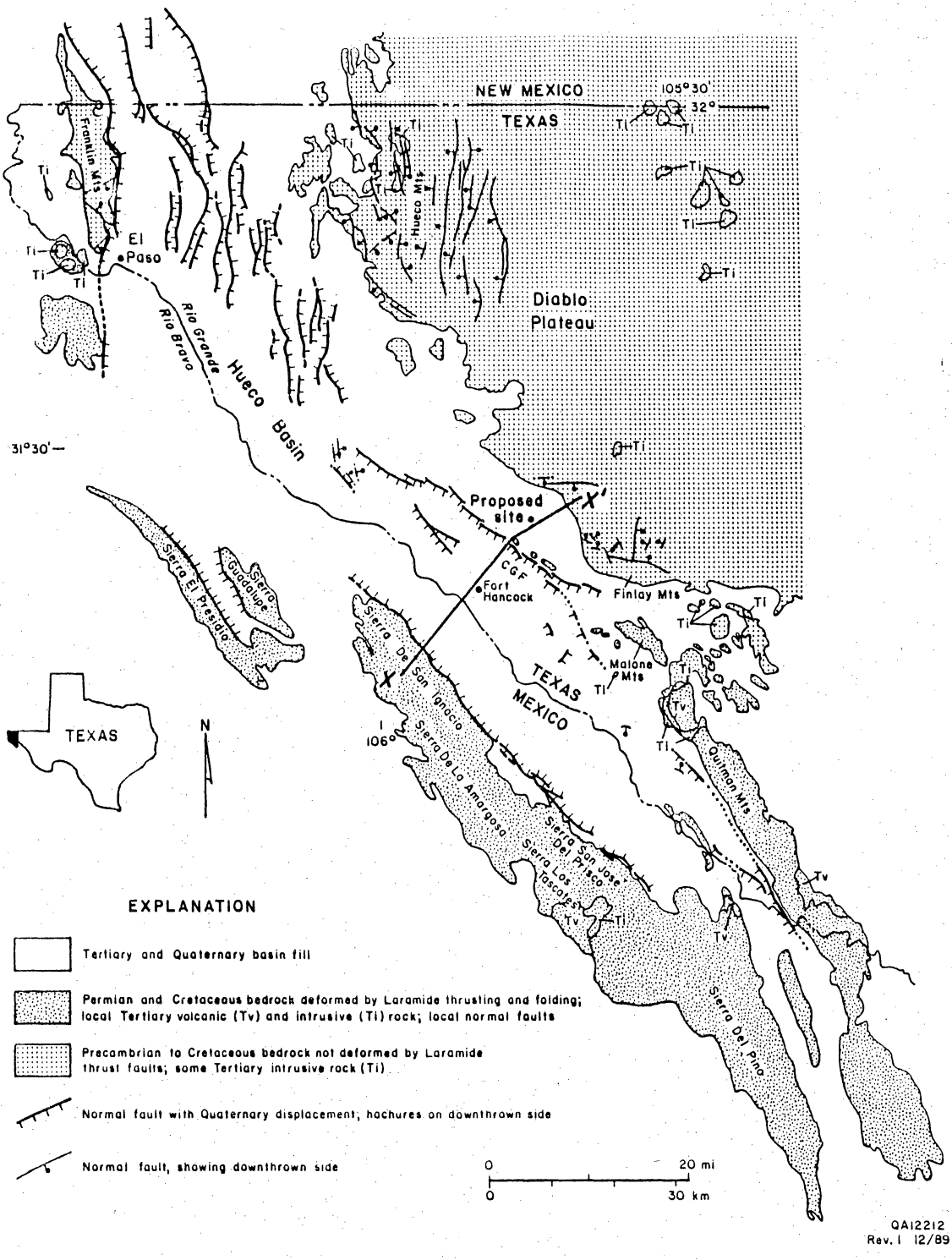

Figure 1. Regional map of surface Quaternary faults (hachures), Hueco Basin, Trans-Pecos Texas. It is unknown if some of the other normal faults (bars) in the region have moved during the Quaternary. CGF = Campo Grande fault. Map was compiled from Albritton and Smith (1965), Jones and Reaser (1970), Woodward and others (1978), Seager (1980), Henry and Price (1985), Dietrich and others (1983), and field and aerial photograph mapping done for this study. See figure 3 for cross section X-X′. Note that scale of regional map prevents some fault strands of Campo Grande fault system from being shown. See figure 2 and plate 1 for detail.

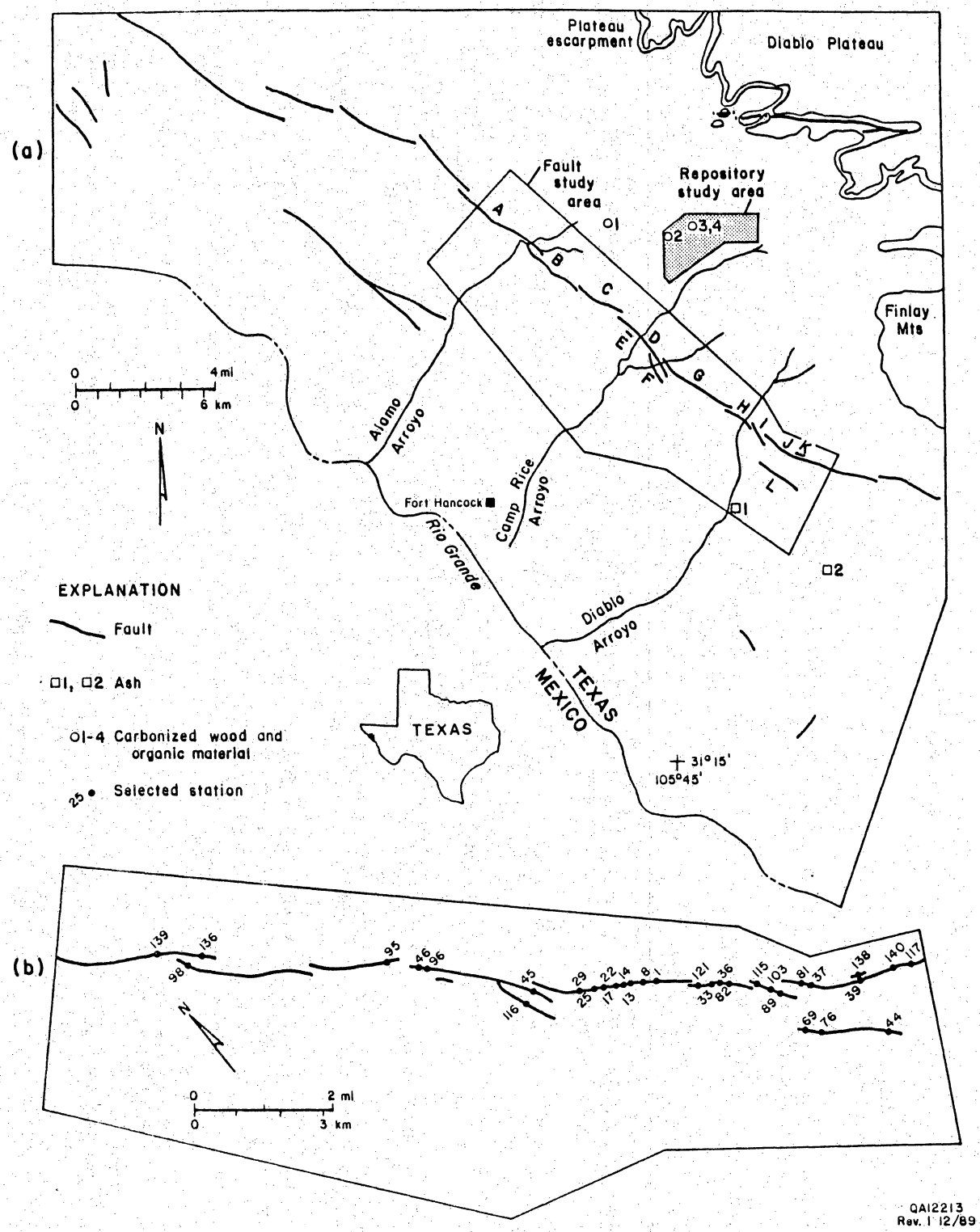

QA12213
Rev. 1 12/89

Figure 2. (a) Map showing study area, proposed waste repository site, locations of dated ash and carbonized material near study area, and en echelon fault strands that compose the Campo Grande fault. A through K identify specific fault strands discussed in this report. Only the western branch of Diablo Arroyo (identified as Campo Grande Arroyo on some maps) is shown. Boundaries of proposed repository study site are approximate. Plate 1 illustrates the detailed geology of the fault study area. (b) Locations of selected stations discussed in this report. Table 1 lists types of data collected at stations.

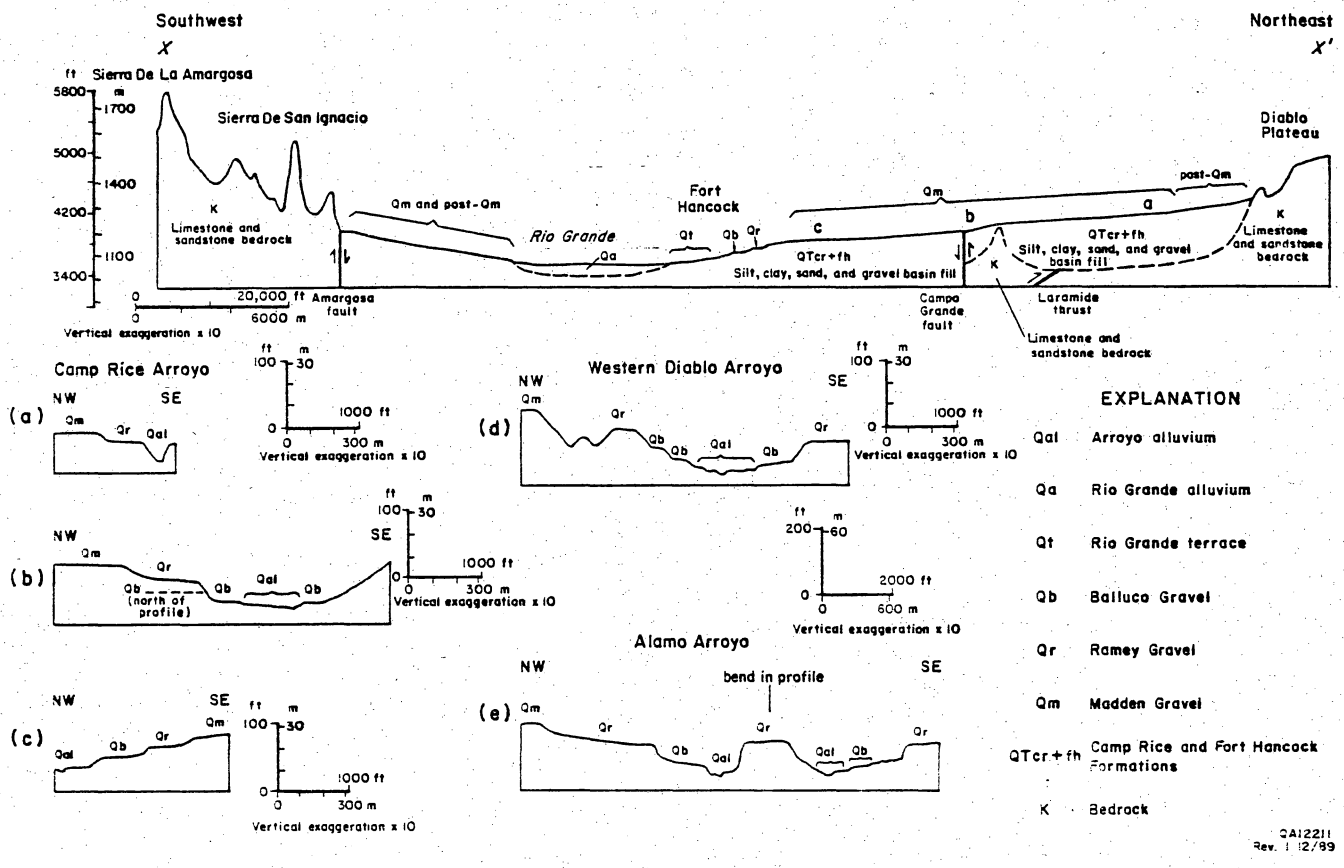

Figure 3. Cross section X-X′ across Hueco Basin at the study area. Cross section location is shown in figure 1. Cretaceous (K) rocks of Sierra De La Amargosa and Sierra De San Ignacio are deformed by Laramide thrusting and folding. Basin-fill deposits between the Amargosa fault and Campo Grande fault are 2 to 3 km thick. The northeastern edge of Laramide thrusting is about 4 km northeast of the Campo Grande fault. Cretaceous (K) rocks of the Diablo Plateau are relatively undeformed and flat lying; they dip 5° to 8° southwestward from the plateau escarpment to the Laramide thrust sheet. Basin fill northeast of the Campo Grande fault is as much as 175 m thick. Profiles shown in b, c, and d are located by the corresponding letters on cross section X-X′. Profiles shown in a and e are located southeast and northwest (respectively) of the b location on cross section X-X′.

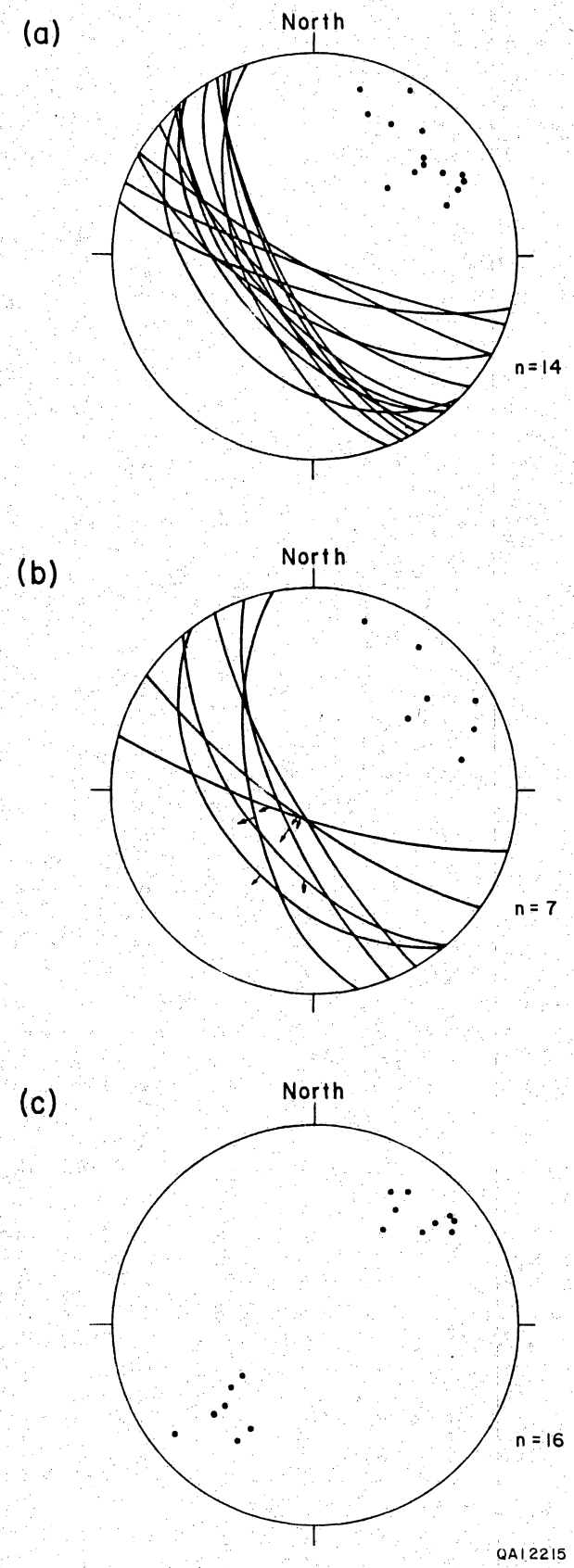

Figure 4. Lower hemisphere, equal-area plots for (a) stereographic projection of fault planes and poles (dots) to fault planes, (b) stereographic projection of fault planes and poles (dots) to fault planes for faults with groove lineations (arrows) on fault plane, and (c) poles of minor-fault planes (minor faults have throws less than 1 m).

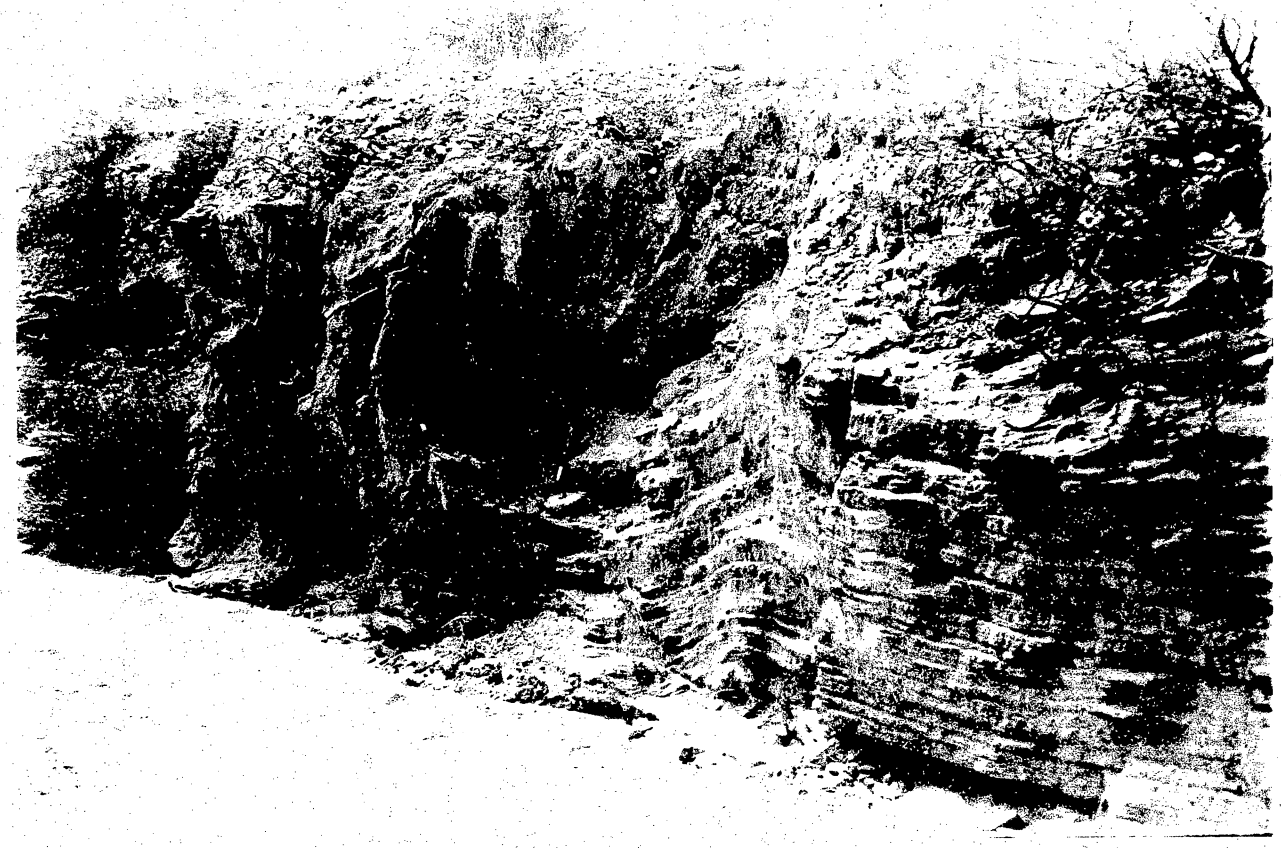

Figure 5. Chaotic folds in Camp Rice sand possibly caused by liquefaction initiated during an earthquake. Location is 1,300 ft (400 m) south of station 44 (fig. 2b). Height of outcrop is about 2 m.

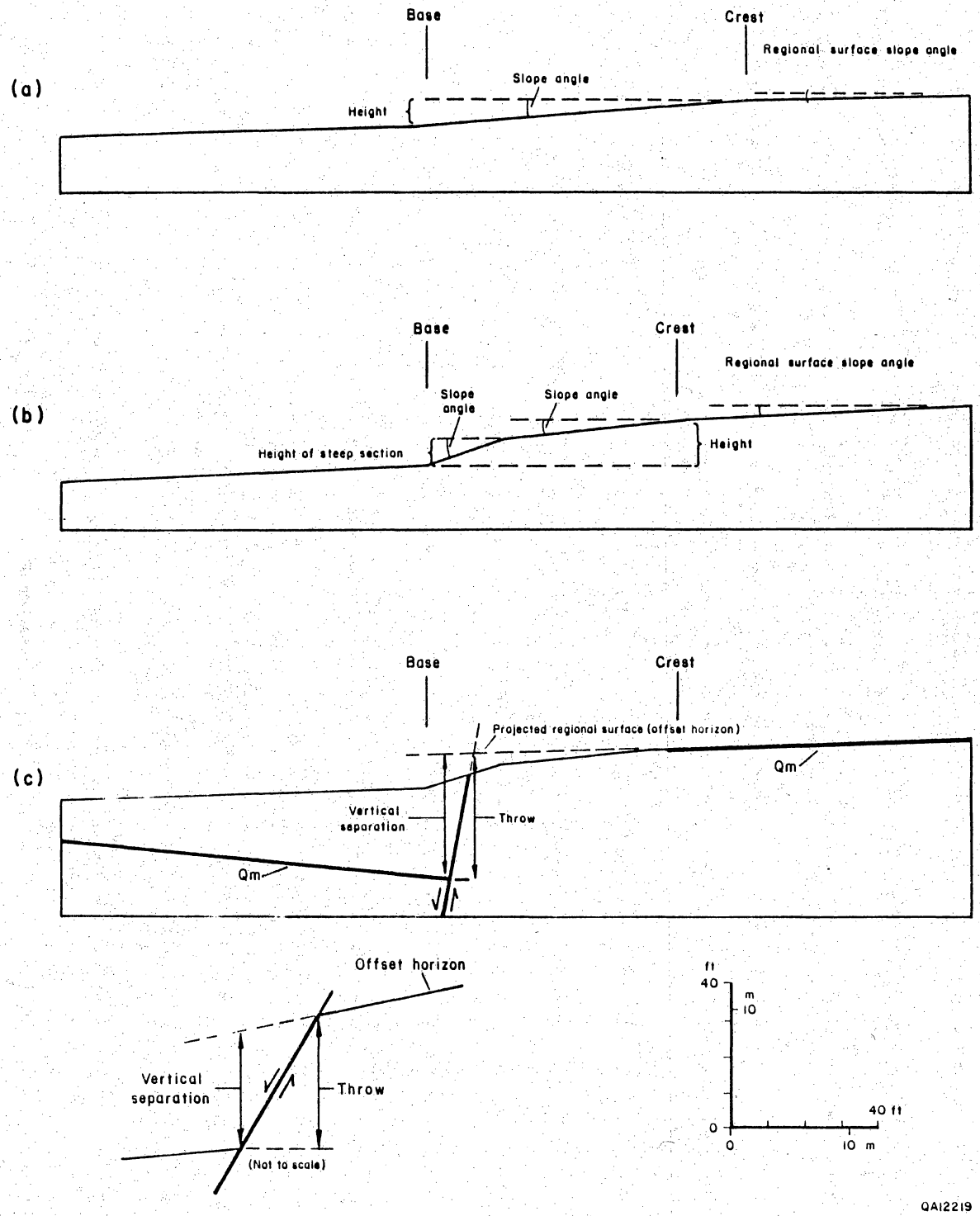

Figure 6. (a) Diagram of single-slope scarp. This type of scarp is common in the Campo Grande fault study area. Profile example is from station 17 (fig. 2b). (b) Diagram of compound-slope scarp (compound scarp). This type of scarp is uncommon in the Campo Grande fault study area. Profile example is from station 14 (fig. 2b). (c) Diagram showing the small difference between throw and vertical separation of a faulted unit at the Campo Grande fault study area. The small difference is caused by low slopes of the offset horizon. Profile example is from station 14 (fig. 2b). Qm = Madden Gravel. Inset example is schematic.

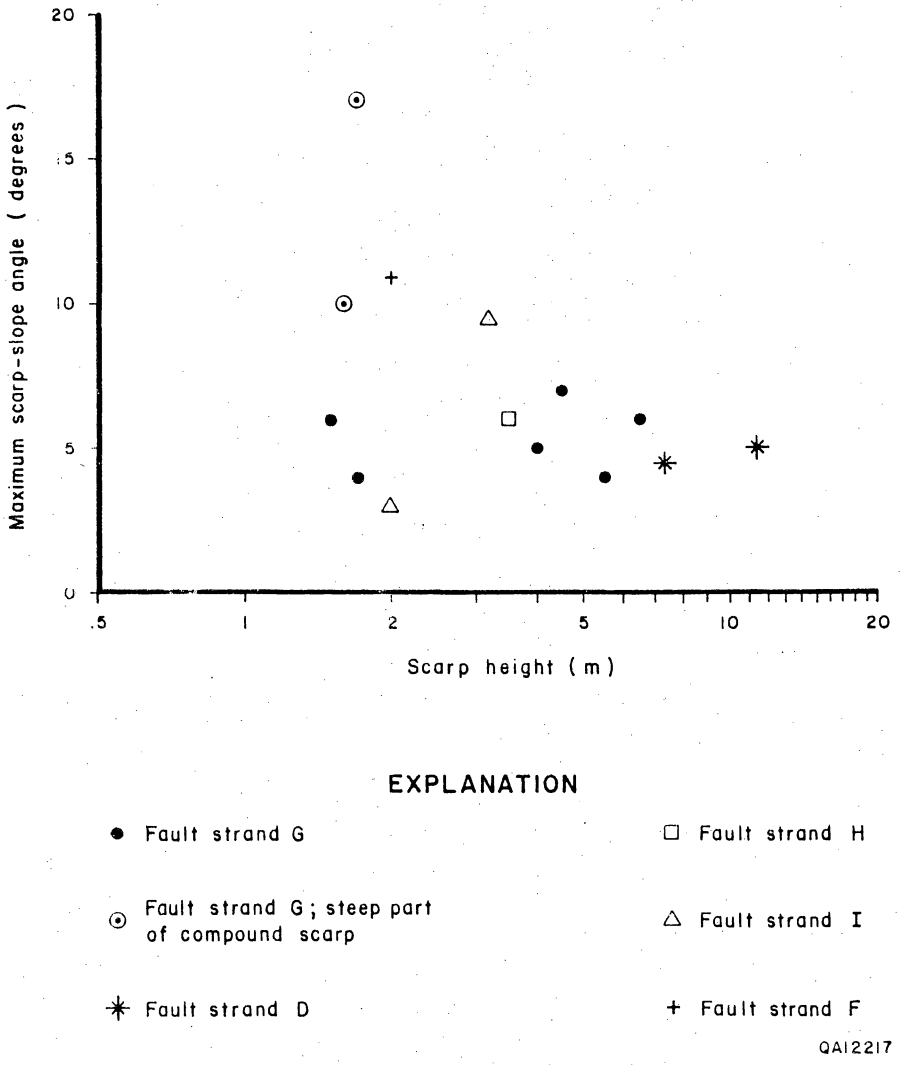

Figure 7. Graph of scarp heights versus maximum scarp-slope angles in the Campo Grande fault study area. Caliche, which is more resistant to erosion than unconsolidated deposits are, is at or near the surface. Fault strands are depicted in figure 2a. Data plotted on graph are reported in table 4.

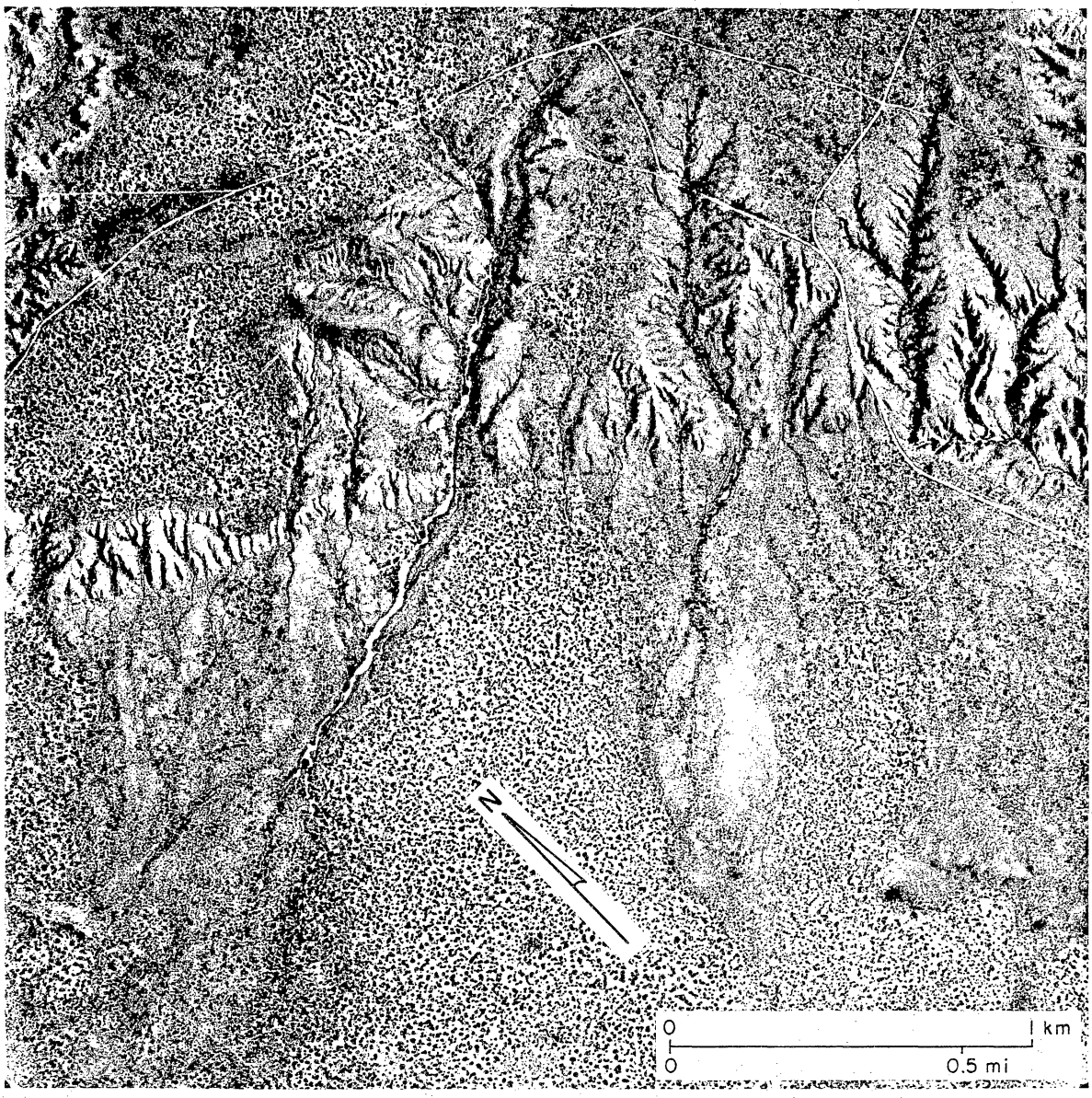

Figure 8a. Aerial photograph (approximate scale 1:12,000) of scarp of fault strand G (fig. 2a). This is the most distinct scarp of the en echelon series of faults that compose the Campo Grande fault.

Figure 8b. Oblique aerial photograph of scarp of fault strand G (northward view). Excavation across scarp is at station 25.

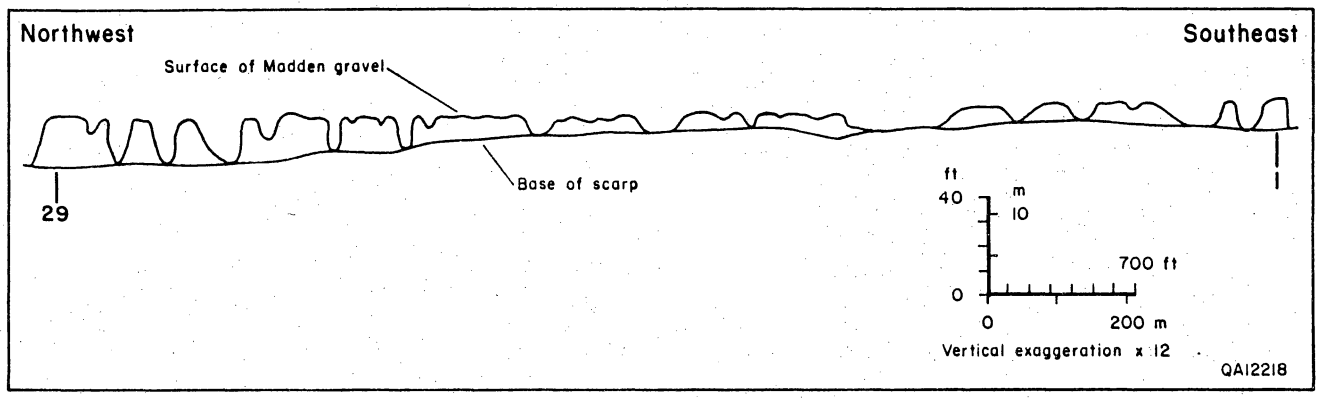

Figure 9. Profile along scarp length of fault strand G between stations 1 and 29 (fig. 2). View is northeastward.

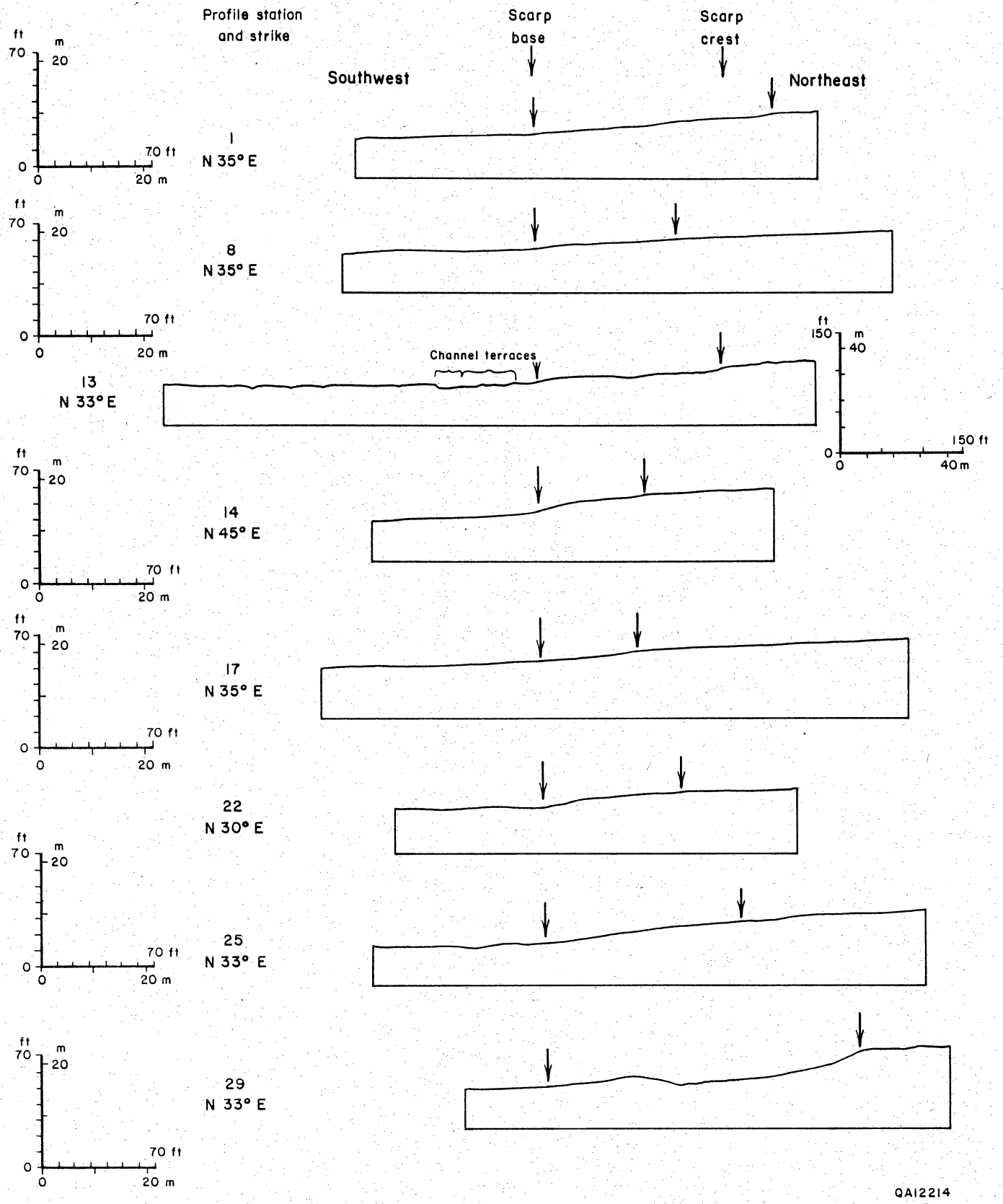

Figure 10. Profiles of scarp of fault strand G illustrating the small scarp-slope angles and profile variations that occur along the scarp. In many places only slight changes in slope and uneroded, flat-lying caliche determine the location of the scarp crests.

Figure 11. Photograph of fault scarp along part of fault strand G near station 22 (fig. 2). View is north-northwestward; stations 25 and 29 are on scarp at left end of photograph.

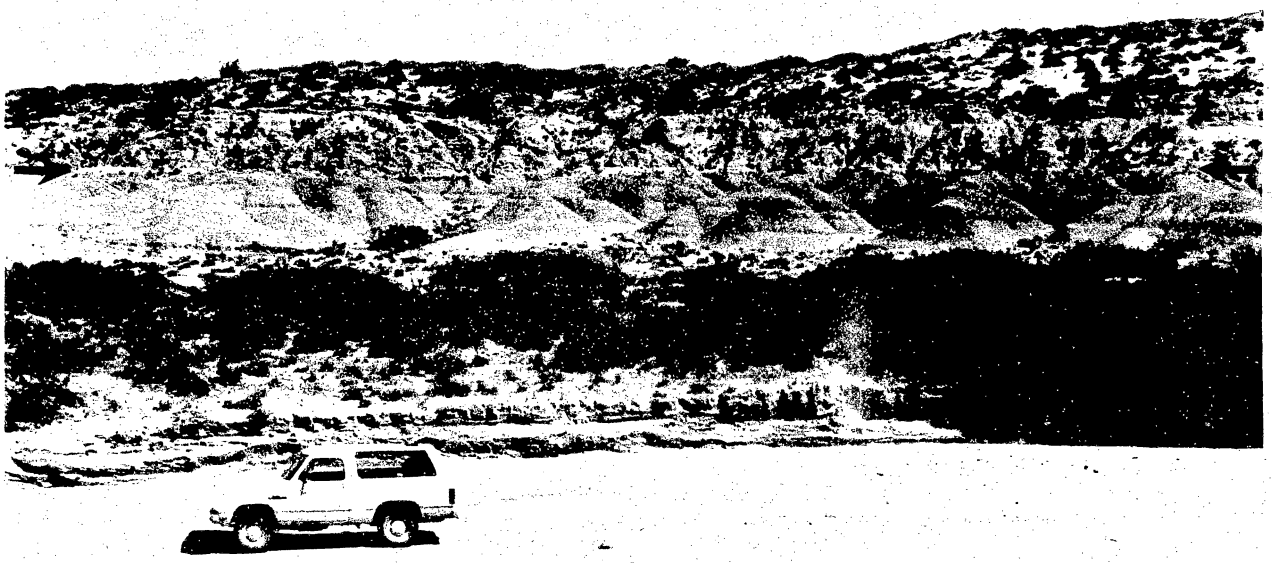

Figure 12. Angular unconformity (arrows) between Fort Hancock Formation (Tfh) and Camp Rice Formation (QTcr). Outcrop is located in Alamo Arroyo about 650 ft (200 m) north of station 139 (fig. 2b).

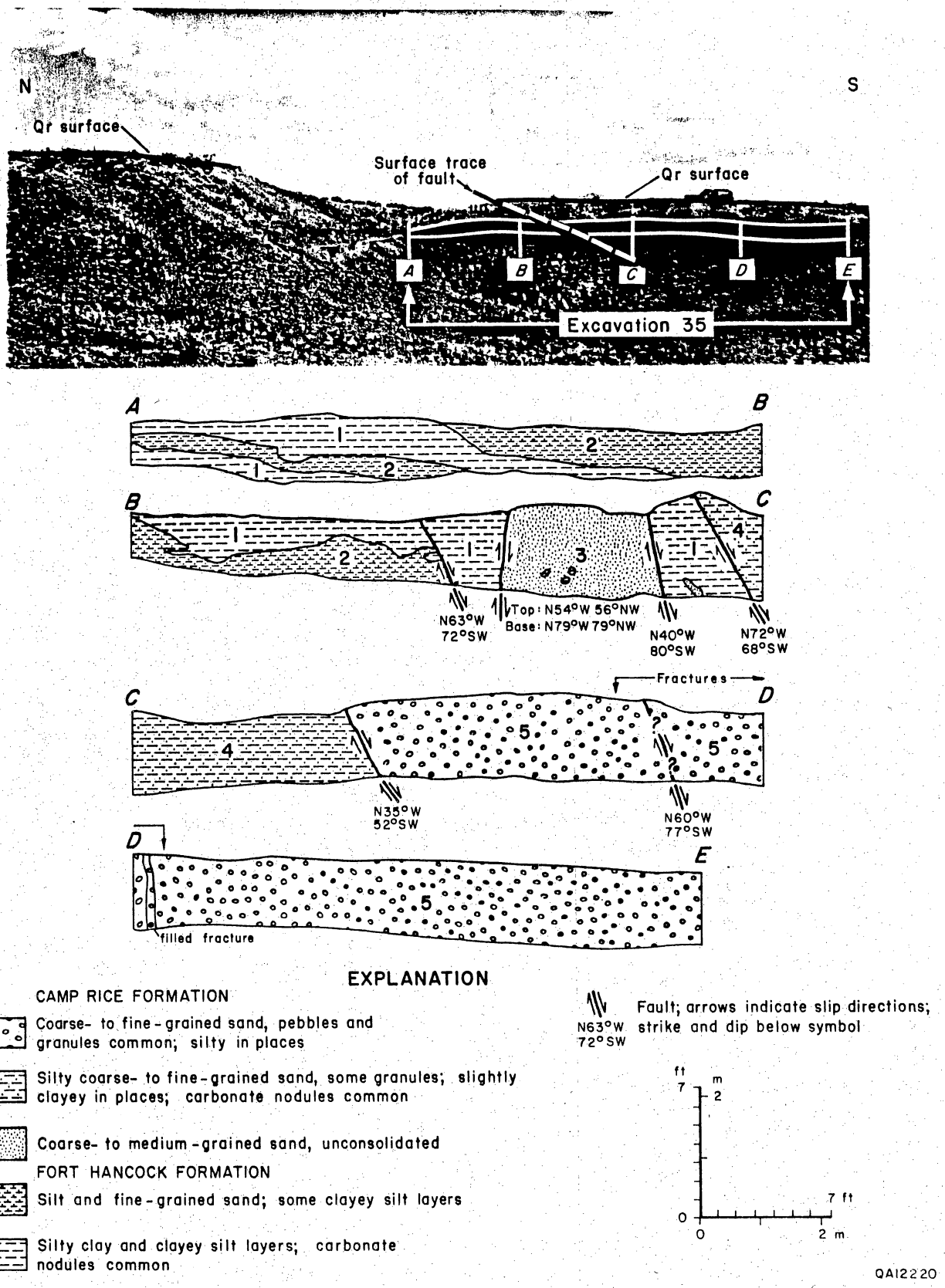

Figure 13. Photograph of offset Ramey Gravel (Qr) and sketch of faults at excavation 35 (fig. 2b, station 35). Ramey Gravel (Qr) on hanging wall is slightly tilted and dips about 5° south-southeastward. Strike of excavation 35 is N80°E (oblique to faults). View of photograph is south-southeast.

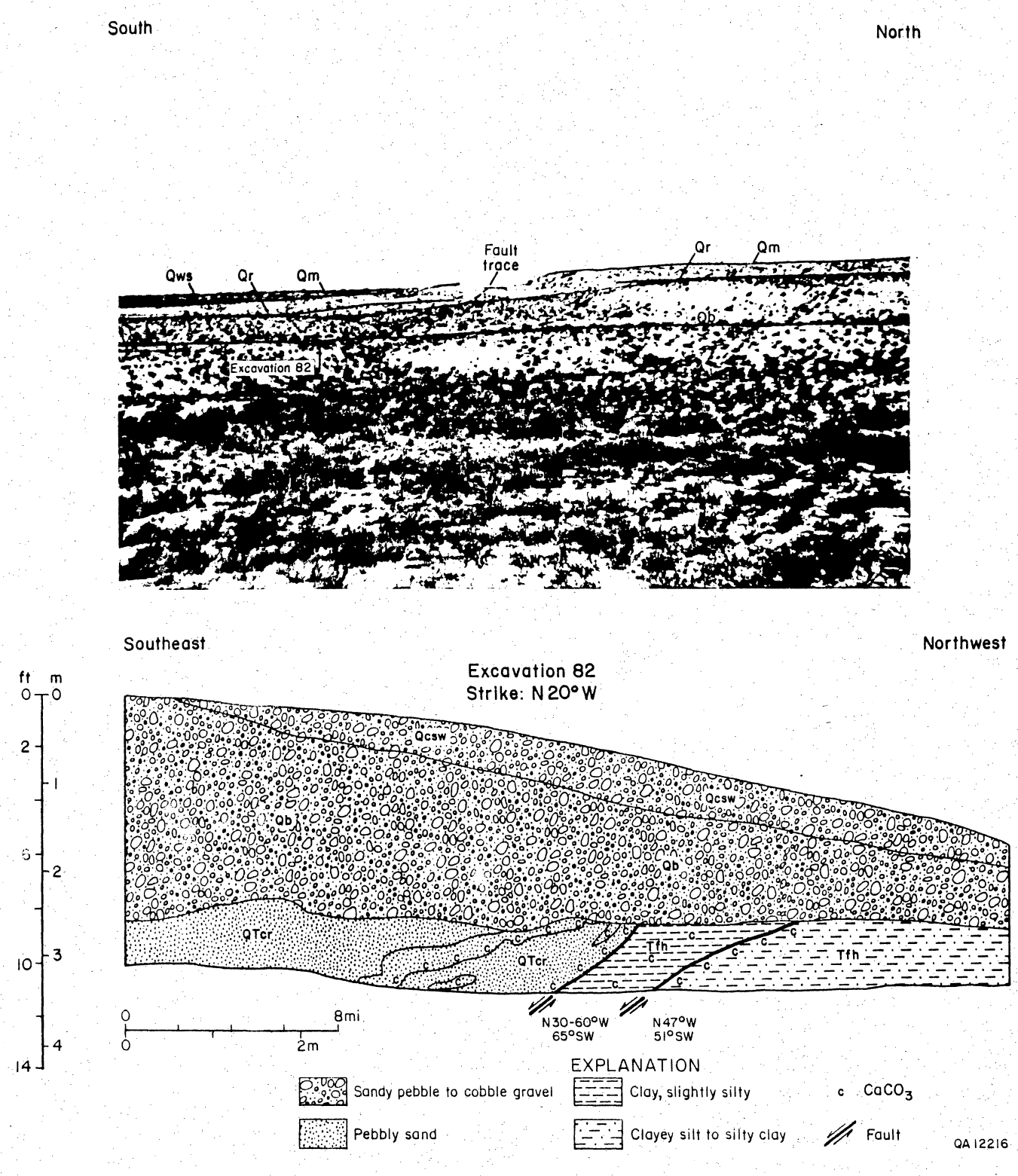

Figure 14. Photograph of offset Madden (Qm) and Ramey (Qr) Gravels, unfaulted Balluco Gravel (Qb), and sketch of excavation 82 (fig. 2b, station 82) illustrating unfaulted Balluco Gravel overlying faults. Qws = windblown sand; Qcsw = colluvium and/or slopewash. Photograph view is south-southwest.

Figure 15. Photograph of channel that has been cut into Camp Rice Formation and filled with younger (Holocene?) alluvium. Outcrop location is approximately 500 ft (150 m) south of station 139 (fig. 2b). Staff is 1 m long.

APPENDIX: OUTCROP SKETCHES OF FAULTS AND FRACTURES

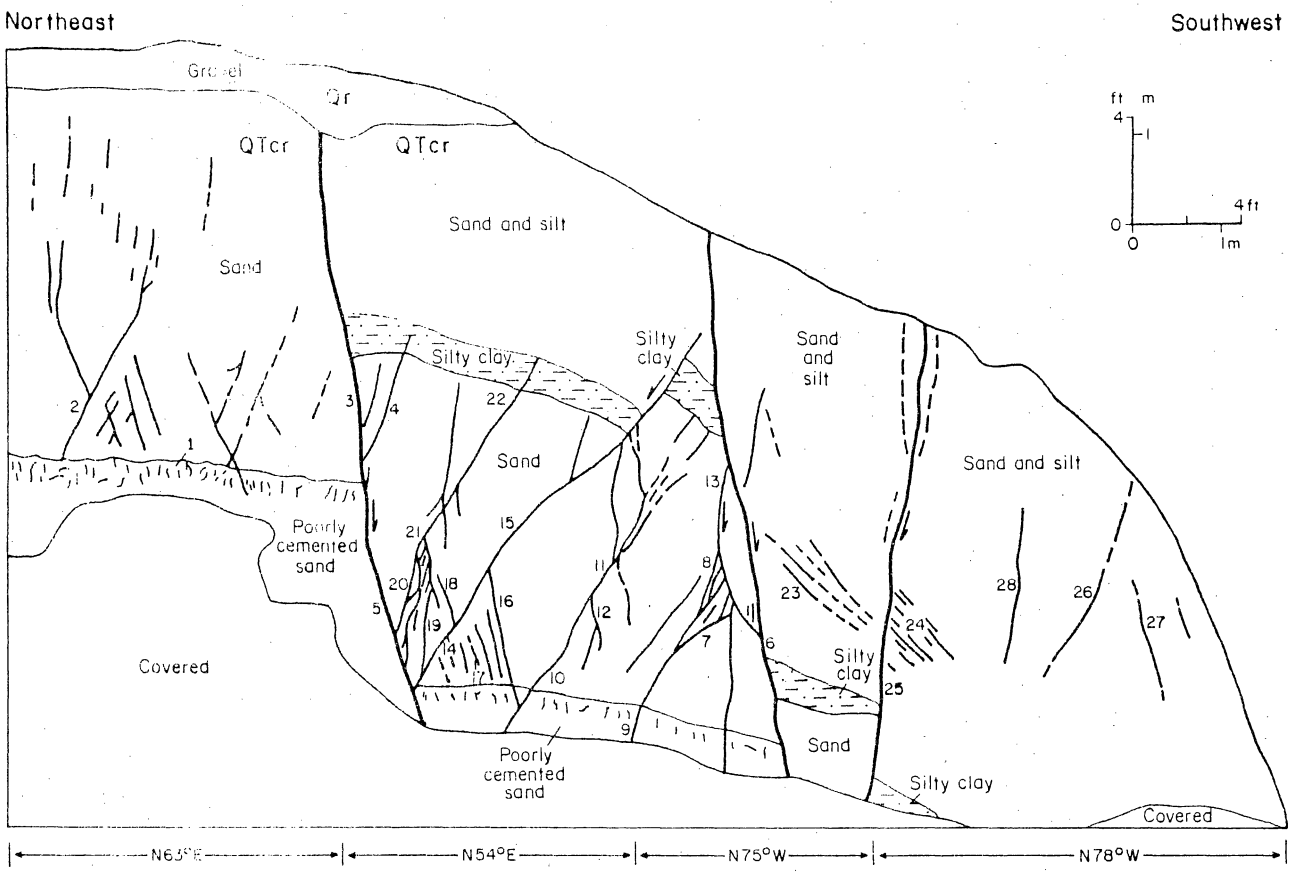

EXPLANATION

1 Vuggy weathering below contact between poorly cemented, medium- to coarse-grained sand and overlying better cemented, medium- to coarse-grained sand

2 Fracture. N30°W 64°NE

3 Fault I. N33°W 79°SW. 2.3-m throw; 20-cm-wide fault zone consists of closely spaced fractures; zone narrows to 8 cm where footwall is poorly consolidated sand

4 Fracture. N28°W 64°NE

5 Fault I. N29°W 73°SW

6 Fault II. N7°E 81°W to N5°W 77°W. 3-m throw; small fault bounding adjacent 40-cm-wide fault wedge strikes N10°W and dips 70 to 59°W

7 Fracture. N12°E 20 to 45°E

8 Fracture. N7°W 82 to 60°E

9 Fracture. N8°W 50°E

10 Fracture. N15°W 80°E

11 Fracture. N10°W 61°E

12 Fracture. N24°W 76°W

13 Fracture. N4°W 76°E

14 Fracture. N19°W 52°E

15 Fracture. N9°W 58°E

16 Fracture. N10°W 73°W

17 Fracture. N21°W 73°W

18 Fracture. N22°W 75°W

19 Fracture. N12°W 87°E

20 Fracture. N22°W 65°E

21 Fracture. N5°W 80°E

22 Fracture. N7°W 52°E

23 Fracture. N22°W 49°W

24 Fractures. Strikes vary from N40 to 50°E; dips vary from 50 to 58°W

25 Fault III. Strike varies from N1°E to N5°W; dip varies from 80°E to 88°W; 0.8-m throw

26 Fracture. N20°W 70°E

27 Slump-related fractures. N22°E 71°W

28 Fracture. N24°W 76°E to89°W

QA12258
Rev. I 12/89

Figure A-1. Outcrop sketch of faults and fractures at station 44 (fig. 2b). QTcr = Camp Rice Formation; Qr = Ramey Gravel.

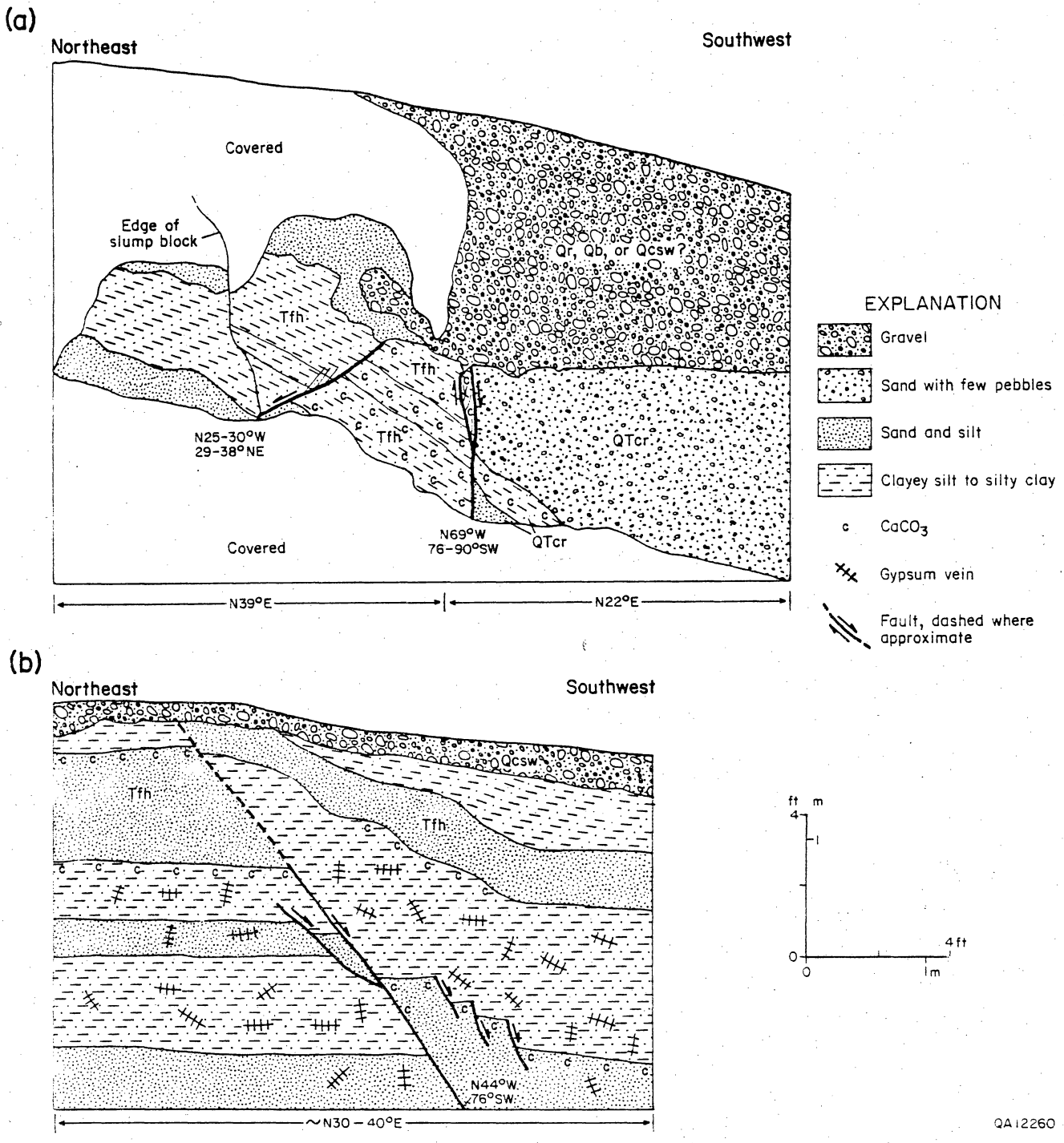

Figure A-2. Outcrop sketches of (a) faults at station 39 and (b) faults at station 138 (fig. 2b). Tfh = Fort Hancock Formation; QTcr = Camp Rice Formation; Qr = Ramey Gravel; Qb = Balluco Gravel; Qcsw = colluvium and/or slope wash alluvium.

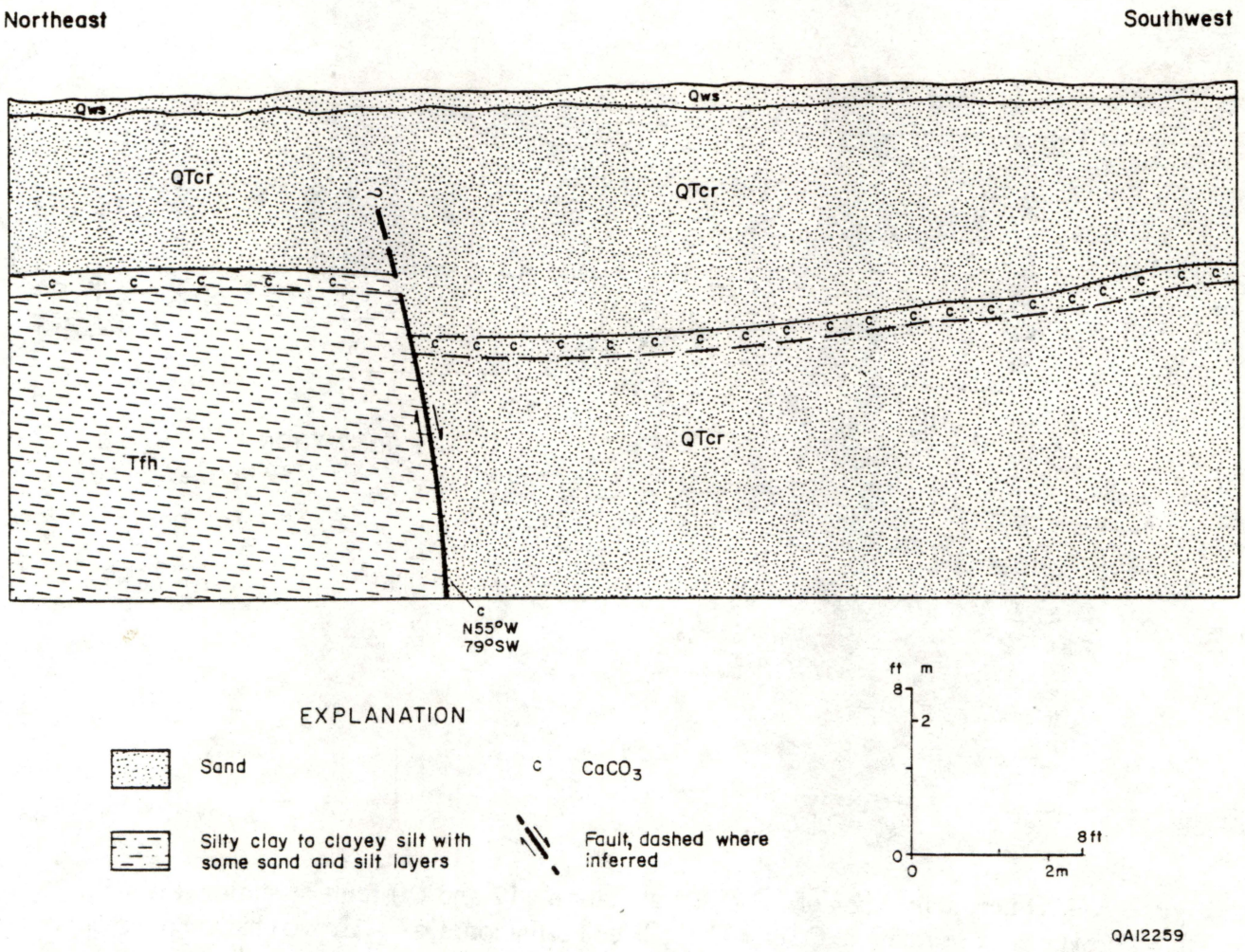

Figure A-3. Outcrop sketch of fault at station 136 (fig. 2b). Angular unconformity occurs between Fort Hancock and Camp Rice deposits. $CaCO_3$ occurs along fault plane. Tfh = Fort Hancock Formation; QTcr = Camp Rice Formation; Qws = windblown sand.

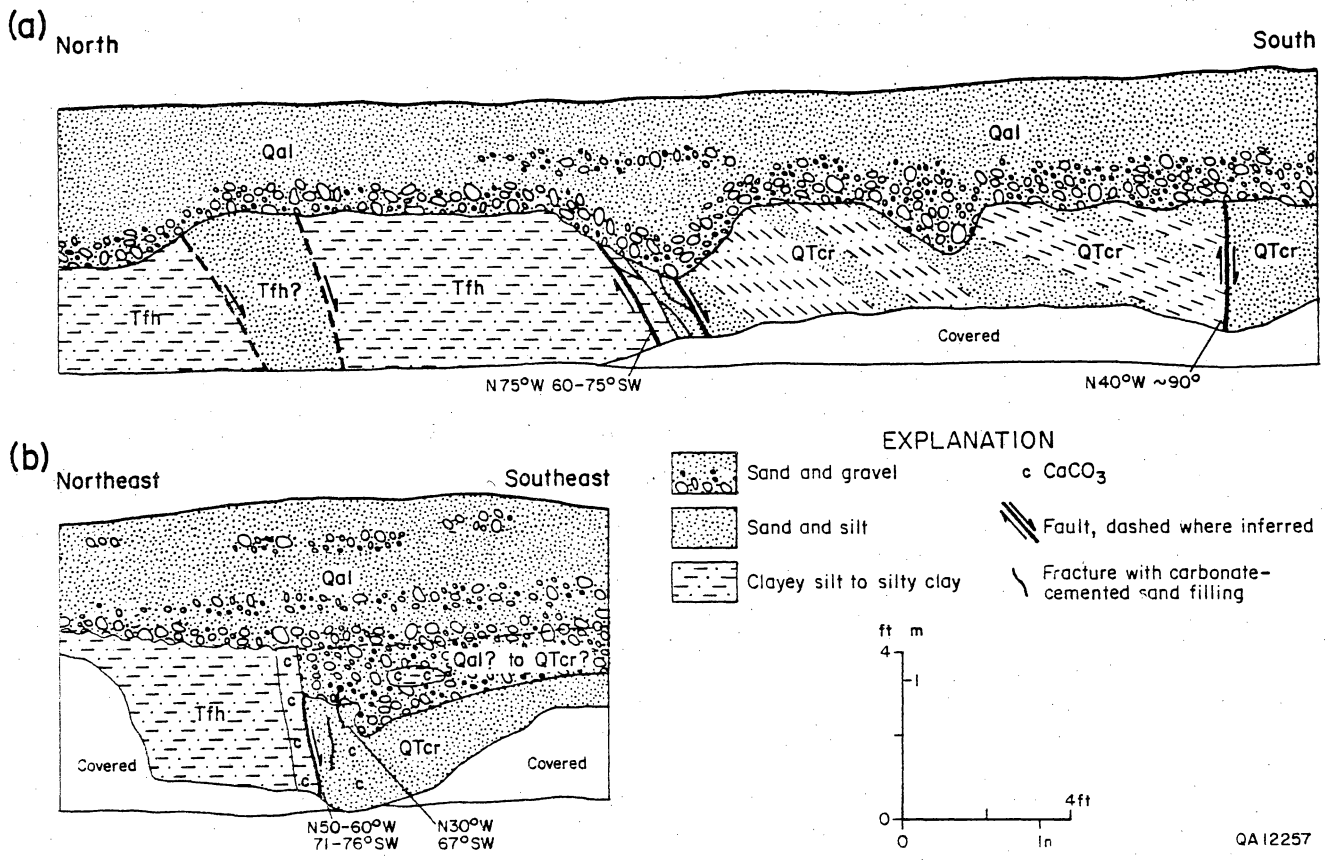

Figure A-4. Outcrop sketches of (a) faults at station 117 and (b) fault at station 139 (fig. 2b). Tfh = Fort Hancock Formation; QTcr = Camp Rice Formation; Qal = Arroyo channel or associated low-terrace alluvium.

Table 1. Types of data collected at selected stations.*

Selected station	Scarp morphology profile	Outcrop sketch	Excavation log	Fault-plane characteristics	Profile for Qm offset†
1	+				+
8	+		+		
13	+				
14	+		+	+	+
17	+				
22	+				
25	+		+	+	
29	+				
33				+	
35	+		+	+	
37				+	
39		+		+	
44		+		+	
45					+
46	+				
69					+
76					+
81				+	
82			+	+	
89				+	
95					+
96	+				+
98				+	
103	+				+
115	+				+
116	+				+
117		+		+	
121					+
136		+		+	
138		+		+	
139		+		+	
140					+

*Station numbers correspond to locations depicted in figure 2b.

†Borehole data used in conjunction with topographic profile data at some locations.

Table 2. Stratigraphy of the Hueco Basin study area and south-central New Mexico.

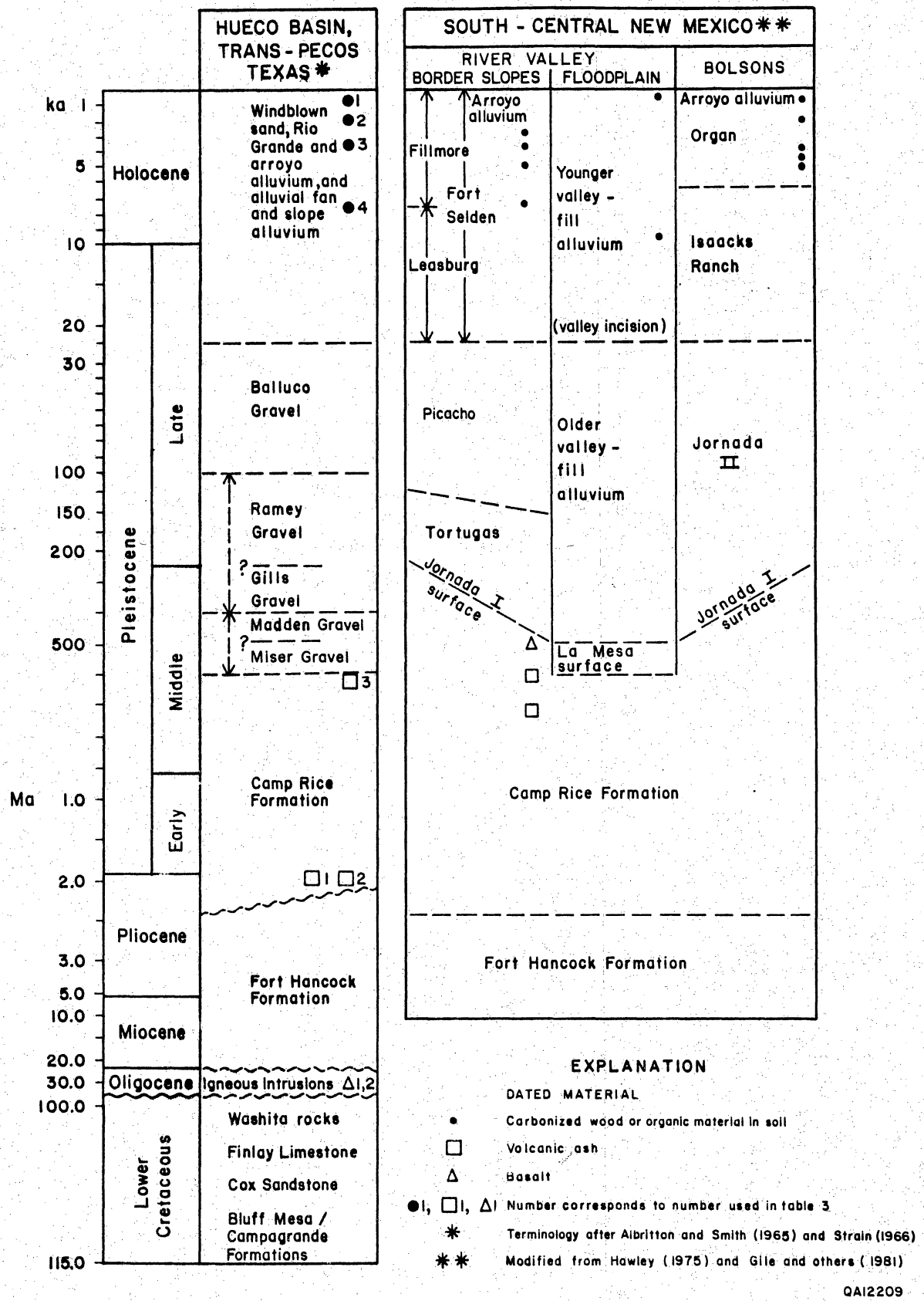

Table 3. Dated material at and near Campo Grande fault study area, Hueco Basin, Trans-Pecos Texas.*

Material	Number	Date	Analysis	Location	Reference
carbonized wood	1	970 ± 20	C-14	upper Alamo Arroyo	R. Baumgardner (personal communication, 1988)
organic material in soil	2	1,330 ± 60	C-14	upper Alamo Arroyo	R. Baumgardner (personal communication, 1989)
organic material in soil	3	3,240 ± 230	C-14	proposed repository study area	R. Baumgardner (personal communication, 1989)
organic material in soil	4	7,510 ± 100	C-14	proposed repository study area	R. Baumgardner (personal communication, 1989)
ash (Huckleberry Ridge)	1	2.1 Ma	see reference	Diablo Arroyo, Hudspeth Co., TX	Izett and Wilcox (1982)
ash (Huckleberry ridge)	2	2.1 Ma	see reference	Madden Arroyo, Hudspeth Co., TX	Izett and Wilcox (1982)
ash (Lava Creek B)	3	0.6 Ma	see reference	El Paso, El Paso Co., TX	Izett and Wilcox (1982)
basalt	1	29.4 ± 1.1 Ma 34.1 ± 0.7 Ma	K-Ar	basalt intrusion approximately 3 to 5 mi (5 to 8 km) west of Quitman and Malone Mountains	Henry and others (1986)
felsic intrusion	2	40.7 ± 2.5 Ma	K-Ar	Finlay Mountains	Matthews and Adams (1986)
mafic to felsic intrusion	2	46.9 ± 1.2 Ma 47.2 ± 1.2 Ma 47.5 ± 2.5 Ma	K-Ar	Finlay Mountains	Henry and others (1986)

*Numbers correspond to those in table 2.

Table 4. Morphometric data for scarps of Campo Grande fault strands.*

Profile station	Regional slope angle (degrees)	scarp slope (degrees)	Total scarp height (m)	Compound Scarp: Steep section slope (degrees)	Steep section height (m)	Less steep section slope (degrees)	Less steep section height (m)	Comments
P-1	2.5	5.0	4.0	—	—	—	—	Scarp on Qm; alluvium covers hanging-wall block; fault strand G.
P-8	1.0	4.0	1.7	—	—	—	—	Scarp on Qm; windblown sand covers hanging-wall block and part of foot wall block; fault strand G.
P-13	2.5	4.0	5.5	—	—	—	—	Scarp on Qm; alluvium covers hanging-wall block; fault strand G.
P-14	2.5	—	3.7	17.0	1.7	6.0	2.0	Scarp on Qm; alluvium covers hanging-wall block; fault strand G.
P-17	2.0	6.0	1.5	—	—	—	—	Scarp on Qm; alluvium covers hanging-wall block; fault strand G.
P-22	1.5	—	2.5	10.0	1.6	4.0	0.9	Scarp on Qm; alluvium covers hanging-wall block; fault strand G.
P-25	3.0	7.0	4.5	—	—	—	—	Scarp on Qm; alluvium covers hanging-wall block; fault strand G.
P-29	2.5	6.0	6.5	—	—	—	—	Scarp on Qm; alluvium covers hanging-wall block; fault strand G.
P-36	1.0	6.0	3.5	—	—	—	—	Scarp on Qr; fault strand H.
P-46	1.5	5.0	11.5	—	—	—	—	Scarp on Qm; scarp very dissected and eroded; fault strand D.
P-96	1.5	4.0	7.3	—	—	—	—	Scarp on Qm; alluvium covers hanging-wall block; fault strand D.
P-103	2.0	9.5	3.2	—	—	—	—	Scarp on Qr; fault strand I
P-115	1.5	3.0	2.0	—	—	—	—	Scarp on Qr; thin alluvium deposits cover hanging-wall block; fault strand I.
P-116	3.0	11.0	2.0	—	—	—	—	Scarp on Qm; fault strand F.

*Station numbers correspond to those in figure 2.

Table 5. Relationships between Quaternary units and faults.*

Fault strand	Chronostratigraphic relationships			
	Qm	Qr	Qb	Qal
A	Scarp indicates vertical offset; amount of offset unknown; scarp covered by windblown sand.	No vertical offset based on absence of scarp.	No vertical offset based on absence of scarp.	No offset based on unfaulted Qal overlying fault and absence of scarp.
B	Scarp indicates vertical offset; amount of offset unknown; scarp covered by windblown sand.	No vertical offset based on absence of scarp.	Strand does not intersect Qb.	No vertical offset based on absence of scarp.
C	Scarp indicates vertical offset; scarp covered by windblown sand; at least 8 m throw on Qm caliche based on measurements from gully outcrops and shallow augerholes.	Strand does not intersect Qr.	Strand does not intersect Qb.	No vertical offset based on absence of scarp.
D	Scarp indicates vertical offset; 10 m throw based on measurements from gully outcrops and shallow augerholes; throw near eastern termination south of Finlay Tank is 3.7 m where Qm of downthrown block dips 12° NE (maximum) toward fault.	Not faulted.	No vertical offset based on absence of scarp.	No vertical offset based on absence of scarp.
E	Scarp indicates vertical offset; amount of offset unknown; scarp covered by windblown sand.	Strand does not intersect Qr.	Strand does not intersect Qb.	—
F	Scarp indicates vertical offset; much of scarp covered by windblown sand; 1.3 m throw measured at one locality.	Strand does not intersect Qr.	Strand does not intersect Qb.	No vertical offset based on absence of scarp.

Table 5 (cont.)

G	Scarp indicates vertical offset; 9 to 10 m throw based on measurements from gully outcrops, excavations, and shallow augerholes; Qm of downthrown block dips NE toward fault; localized tilting of younger calcic horizons which dip SW away from fault; throw near eastern termination is 1 to 1.5 m.	Strand does not intersect Qr.	Strand does not intersect Qb.	No vertical offset based on absence of scarp.
H	Dissected scarp indicates vertical offset; 6 m throw based on measurements from outcrop; strata on downthrown block dips 5 to 7° SW, away from fault.	Scarp indicates vertical offset; 3 m throw based on measurements from outcrop and an excavation.	No offset based on unfaulted Qb overlying fault and absence of scarp.	No vertical offset based on absence of scarp.
I	Strand does not intersect Qm.	Scarp indicates vertical offset; 2.6 m throw based on measurements from outcrops.	Strand may not intersect Qb; Qb west of fault has no scarp.	No vertical offset based on absence of scarp.
J	Dissected scarp indicates vertical offset; 9 m throw based on measurements from outcrop.	No offset based on unfaulted Qr overlying fault and absence of scarp.	Strand does not intersect Qb.	No vertical offset based on unfaulted Qal overlying fault and absence of scarp.
K	Strand does not intersect Qm.	No offset based on unfaulted Qr overlying fault and absence of scarp.	Strand does not intersect Qb.	No vertical offset based on absence of scarp.
L	Scarp indicates vertical offset; 1 to 2 m throw based on measurements from outcrop.	No offset based on unfaulted Qr overlying fault and absence of scarp.	No vertical offset based on absence of scarp.	No vertical offset based on absence of scarp.

*Fault strand locations are shown in figure 2.
Qm = Madden Gravel, Qr = Ramey Gravel, Qb = Balluco Gravel, Qal = Arroyo Alluvium and associated low terraces.

Table 6. Vertical separations between tops of overlying calcic horizons (a to e; e is Qm caliche) on the downthrown fault block and between tops of youngest faulted calcic horizons and the possible "last-event" scarp.*

Location	Number of calcic horizons on hanging wall fault block	Vertical separation (m)	
		Top of possible "last-event scarp" to youngest faulted calcic horizon	Calcic horizons (a = youngest)
Excavation 14 (west wall)	5	1.3	a to b = 1.6 b to c = 1.1 c to d = 2.2 d to e† = 1.5
Excavation 14 (east wall)	5	1.1	a to b = 1.2 b to c = 1.1 c to d = 2.2 d to e‡ = 1.5
Excavation 25 (west wall)	3†	—	a to b = 1.1 b to c = 1.3
Station 45	2	2.0	a to b = 1.5

*Excavations 14 and 25 are illustrated in plates 2a and b.

† More calcic horizons exist at depth.

‡ Projected from augerhole near station 1, southeast of excavation at station 14.